

# Asymmetric bistable systems subject to periodic and stochastic forcing in the strongly nonlinear regime: Switching time distributions

A. Nikitin,<sup>1</sup> N. G. Stocks,<sup>1</sup> and A. R. Bulsara<sup>2</sup><sup>1</sup>*School of Engineering, University of Warwick, Coventry CV4 7AL, United Kingdom*<sup>2</sup>*Space and Naval Warfare Systems Center 2363, 49590 Lassing Road, RM 341, San Diego, California 92152-6147, USA*

(Received 4 November 2002; published 11 July 2003)

A detailed theoretical analysis of the dynamics of a sinusoidally driven noisy asymmetric bistable system is presented. The results are valid for any two-state system, however, the specific case of the Duffing potential is considered in detail. The dynamics are considered in the weak noise limit, i.e., when the response of the system to the external periodic field is strongly nonlinear. The system asymmetry is created by a nonzero dc component of the external force, and manifests itself as an asymmetry between the mean switching times between the potential wells. We obtain explicit analytic expressions for the whole hierarchy of switching time distributions (including the residence time and return time distributions). We also obtain expressions for the average residence times and describe how they depend on asymmetry, together with an explicit expression for the difference between the residence times in the weak noise limit; the results are presented in the context of using the switching dynamics to detect weak dc target signals.

DOI: 10.1103/PhysRevE.68.016103

PACS number(s): 02.50.Ey, 05.45.-a, 85.25.Dq

## I. INTRODUCTION

The phenomenon of stochastic resonance (SR) [1] has stimulated series of theoretical work on the dynamics of bistable systems subject to both a time periodic and noisy driving. However, the vast majority of these studies have concentrated on symmetric systems. Symmetry implies that, on an average, the time the system spends in the two possible stable steady states are equal. Clearly, in many real world situations, symmetry cannot be assumed. Indeed the modification of the dynamics due to asymmetry has been proposed as a means of detecting weak dc target signals using nonlinear dynamical systems, e.g., fluxgate magnetometers and superconducting quantum interference devices [2–6]. It is, therefore, of some importance to investigate the response of such systems particularly in the regime wherein the dc signal introduces the most marked changes in the response.

In this and a following paper [7], we undertake a detailed theoretical analysis of the effect of asymmetry on the dynamics of a bistable system. In contrast to existing studies of symmetric bistable systems (see references in Ref. [1] for numerous examples) only a small number of studies have considered the effect of system asymmetry. Possibly the first asymmetry-mediated effect to be reported was the occurrence of spectral harmonics at even multiples of the forcing frequency [8] in the weakly nonlinear (or SR) regime. The spectral properties of the response of these systems have been exhaustively studied [2–4,9–12] together with the residence time distributions [9]. Recent work has also considered the role of the potential symmetry in a spatially extended bistable system [13].

In this study, we consider the case of the bistable (Duffing) potential subject to a symmetry-breaking dc signal. Our work is an extension of an earlier study [14] wherein the two-state approximation was applied to a periodically driven symmetric bistable system, thereby enabling a simplification of the dynamics through a point-process formulation. The

Duffing system has long served as a generic model for the description of many physical systems [15], but has, more recently, received considerable attention in the context of SR. However, we stress that our central results are applicable to a general bistable system.

We consider the situation wherein the effects of the asymmetry are expected to be at their most pronounced, i.e., when the periodic forcing is strong and the noise is weak. For a general bistable system, the dynamics can be divided into two different regimes where analytical approximations can be obtained: the *linear response regime* and the *nonlinear response regime*. The governing parameter (neglecting any intrawell motion) is the ratio of the amplitude of the external periodic field  $A$  to the noise strength  $D$ . In the limit  $A/D \ll 1$ , the response of the system to the periodic force is approximately linear and hence perturbation theories [16] (using  $A/D$  as a small parameter) and linear response theory [17] can be applied. In the opposite limit,  $A/D \gg 1$ , the response of the system to the external field is highly nonlinear. In this regime, which we consider throughout this work, linear response theories fail and must be replaced by a full nonlinear analysis [9,10,14,15,18]. It is also precisely in this nonlinear regime that the dynamics show many of their richest features such as strong synchronization to the external drive and a double maximum in the signal-to-noise ratio as a function of noise intensity [14]. It is also anticipated that, in this regime, small asymmetries will lead to significant changes in the dynamics.

In an accompanying paper, we consider the effect of asymmetry on the spectral properties of the response [7]. Here, however, we consider the switching time dynamics between the two stable states. For a two-state system, the dynamics can be completely described by a hierarchy of switching time distributions. Indeed, effects such as stochastic resonance have been characterized in terms of residence time distributions [19]. However, it is important to stress that there is a whole hierarchy of such distributions and that the dynamics are only fully specified when all distributions are

known. The hierarchy is formed by considering the time the system takes to make  $j$  switches. The distribution of times associated with a single switch (e.g., state  $1 \rightarrow 2$  or  $2 \rightarrow 1$ ), i.e., when  $j=1$ , is commonly referred to as the residence time distribution. The distribution of times associated with two switches (e.g., states  $1 \rightarrow 2$  and  $2 \rightarrow 1$ , or the opposite sequence), i.e., when  $j=2$ , is commonly referred to as the return time distribution. This idea can be extended to  $j=3,4,\dots$  to give the set of switching distributions  $P_j(\tau)$ . Previous studies of symmetric systems have obtained theoretical expressions for quantities such as the residence time distribution [8,9,14,20] but only one study has obtained explicit analytic expressions for the whole hierarchy of switching time distributions [14]. It is the extension of this study to include asymmetry that we now present.

The paper is organized as follows: after some background material comprising the basic Duffing dynamics and its representation as a discrete two-state system, we compute the switching time distributions (these include the residence as well as the return times distributions introduced above) using an extension of the procedure already utilized earlier [14]. We also compute statistically significant quantities, most importantly the mean values of the residence and return times (in any practical implementation of this procedure, these would be the likely relevant experimental observables), and investigate the effects of the asymmetry on them. We conclude with a discussion of the results, making contact with ongoing work on the efficacy of using the switching times asymmetry as a path towards detecting and quantifying weak dc target signals.

## II. BACKGROUND

### A. Asymmetric Duffing system

We consider the standard overdamped Duffing system subject to an external periodic field  $A \cos(\Omega t)$  and white noise  $\xi(t)$  with intensity  $D$ . The system of equations are given by [15]

$$\dot{x} = -\frac{\partial V(x,t)}{\partial x} + \xi(t), \quad (1a)$$

$$V(x,t) = -\frac{a}{2}x^2 + \frac{b}{4}x^4 + cx - Ax \cos(\Omega t), \quad (1b)$$

$$\langle \xi(t)\xi(t') \rangle = 2D \delta(t-t'), \quad (1c)$$

$$\langle \xi(t) \rangle = 0. \quad (1d)$$

The stochastic equation (1) describes an overdamped particle motion in the bistable potential  $V(x,t)$ . The random barrier hoppings of the particle occur due to noise coupled with a *slow* modulation of the potential by the periodic signal (the particle is assumed to relax to the potential minima after each hopping event).

The extrema of the potential are given by the roots of the equation

$$\frac{\partial V(x,t)}{\partial x} = -ax + bx^3 + c - A \cos(\Omega t) = 0,$$

leading to

$$x_1 = -2 \sqrt{\frac{a}{3b}} \cos \left( \frac{1}{3} \arccos \left[ \frac{A \cos(\Omega t) - c}{2 \sqrt{\left(\frac{a}{3b}\right)^3}} \right] - \frac{\pi}{3} \right), \quad (2)$$

$$x_2 = 2 \sqrt{\frac{a}{3b}} \cos \left( \frac{1}{3} \arccos \left[ \frac{A \cos(\Omega t) - c}{2 \sqrt{\left(\frac{a}{3b}\right)^3}} \right] \right), \quad (3)$$

for the locations of the stable points, and

$$x_s = -2 \sqrt{\frac{a}{3b}} \cos \left( \frac{1}{3} \arccos \left[ \frac{A \cos(\Omega t) - c}{2 \sqrt{\left(\frac{a}{3b}\right)^3}} \right] + \frac{\pi}{3} \right), \quad (4)$$

for the location of the unstable point.

The system asymmetry enters through the parameter  $c$  in  $V(x,t)$ . The symmetric case corresponds to  $c=0$ . In the absence of the periodic field, the potential minima are located symmetrically at  $\pm \sqrt{a/b}$  and the potential barrier height between the points  $x_1, x_s$  and  $x_2, x_s$  are equal and given by  $a^2/4b$ . A nonzero value of  $c$  results in an asymmetric shift in the position of the potential minima and to different barrier heights between the two potential wells. The characteristic relaxation times for the two wells,  $\tau_{rel_1}$  and  $\tau_{rel_2}$ , will also be different [given by  $\tau_{rel_1}^{-1} = V''_{xx}(x_1, t)$  and  $\tau_{rel_2}^{-1} = V''_{xx}(x_2, t)$ ].

The effect of the periodic field is to modulate, i.e., periodically lower and raise, the potential wells. The larger the amplitude  $A$ , the greater the extent of the modulation. For sufficiently large  $A$ , the system will lose the bistable property and become monostable, i.e., the potential wells will periodically vanish in turn.

However, due to the asymmetry, the potential wells will first vanish at different values of the forcing amplitude and will thus have different critical amplitudes  $A_{c1}$  and  $A_{c2}$  for the onset of ‘‘deterministic switching.’’ It is straightforward to show that well  $i$  (i.e., the well positioned at  $x_i$ ) vanishes at  $A_{ci}$  where

$$A_{ci} = \left| c - (-1)^i \frac{2}{3} a \sqrt{\frac{a}{3b}} \right|, \quad i = 1, 2. \quad (5)$$

The theory developed in the following sections is valid for forcing amplitudes smaller than those required to induce deterministic switching—this requires

$$A < \min(A_{c1}, A_{c2}). \quad (6)$$

The theory is valid for forcing amplitude that are *just* insufficient to cause deterministic switching—that is, for forcing amplitudes that are just subthreshold. It is precisely in this regime that the effects of asymmetry are anticipated to be most pronounced. However, it should be stressed that the theory is also valid in the limit  $A \rightarrow 0$  provided the noise intensity  $D$  also goes to zero (at a faster rate), see condition (9) and accompanying discussion.

### B. The two-state approximation

The total dynamics  $x(t)$  can be split into two contributions, an intrawell contribution that arises from motion within the potential wells and an interwell contribution that characterizes the switching between the two states. As we are only interested (in this study) in calculating the switching time distributions, we can neglect the contribution due to intrawell motion. This allows us to replace, fully, dynamics (1) by a reduced two-state model which can be described by a linear rate equation with periodic coefficients [16]:

$$\begin{aligned} \dot{w}_1 &= -[W_{12}(t) + W_{21}(t)]w_1 + W_{21}(t), \\ w_1 + w_2 &= 1, \end{aligned} \quad (7)$$

where  $w_1, w_2$  are the probabilities of being in state 1 and 2, and  $W_{12}(t), W_{21}(t)$  are the transition rates from states 1  $\rightarrow$  2 and 2  $\rightarrow$  1, respectively. Due to the periodic field, we also have the relations

$$\begin{aligned} W_{12}(t) &= W_{12}(t+T), \\ W_{21}(t) &= W_{21}(t+T), \end{aligned}$$

where  $T = 2\pi/\Omega$ .

If  $\Omega \ll \tau_{rel1}^{-1}, \Omega \ll \tau_{rel2}^{-1}$ , then an adiabatic approximation [16] can be used and the transition rates approximated as

$$\begin{aligned} W_{12}(t) &= \frac{\sqrt{|V''_{xx}(x_1(t),t)V''_{xx}(x_s(t),t)|}}{2\pi} \\ &\quad \times \exp\left[\frac{V(x_1(t),t) - V(x_s(t),t)}{D}\right], \\ W_{21}(t) &= \frac{\sqrt{|V''_{xx}(x_2(t),t)V''_{xx}(x_s(t),t)|}}{2\pi} \\ &\quad \times \exp\left[\frac{V(x_2(t),t) - V(x_s(t),t)}{D}\right]. \end{aligned} \quad (8)$$

The expression for the transition rates can be simplified if we impose the condition

$$A/D \gg 1, \quad (9)$$

i.e., the noise is weak compared to the amplitude of the periodic driving force. This condition results in highly nonlinear dynamics referred to, henceforth, as the nonlinear regime; this regime is to be contrasted with the opposite limit  $A/D \ll 1$  in which linear response theories are applicable

[16,17]. It should be stressed that theory developed here is only valid when condition (9) is satisfied. However, we place no restriction on the magnitude of  $A$  other than condition (6).

In the nonlinear regime  $W_{12}$  and  $W_{21}$  are highly peaked at times  $t' = nT$  and  $t' = (n + \frac{1}{2})T$ , respectively ( $n = 0, 1, 2, \dots$ ), and drop close to zero at all other times. This allows the exponents in Eq. (8) to be Taylor expanded in time about  $t' = nT$  and  $t' = (n + \frac{1}{2})T$ . For  $W_{12}$  this gives

$$\begin{aligned} &\exp\left[\frac{V(x_1(t),t) - V(x_s(t),t)}{D}\right] \\ &= \exp\left\{\left(\frac{V(x_1(t'),t') - V(x_s(t'),t')}{D}\right) \right. \\ &\quad + \left(\frac{V'_t(x_1(t'),t') - V'_t(x_s(t'),t')}{D}\right)(t-t') \\ &\quad \left. + \left(\frac{V''_{tt}(x_1(t'),t') - V''_{tt}(x_s(t'),t')}{D}\right)\frac{(t-t')^2}{2} + \dots\right\} \\ &\approx \exp\left[\frac{V(x_1(t'),t') - V(x_s(t'),t')}{D}\right] \exp\left(-\frac{(t-t')^2}{2\delta t_1^2}\right), \end{aligned} \quad (10)$$

where

$$\delta t_1 = \sqrt{\frac{D}{|x_1(t') - x_s(t')| A \Omega^2}}. \quad (11)$$

Similarly,

$$\begin{aligned} &\exp\left[\frac{V(x_2(t),t) - V(x_s(t),t)}{D}\right] \\ &\approx \exp\left[\frac{V(x_2(t'),t') - V(x_s(t'),t')}{D}\right] \exp\left(-\frac{(t-t')^2}{2\delta t_2^2}\right), \end{aligned} \quad (12)$$

where

$$\delta t_2 = \sqrt{\frac{D}{|x_2(t') - x_s(t')| A \Omega^2}}. \quad (13)$$

The transition probabilities can now be rewritten as

$$W_{12}(t) = \sum_{n=-\infty}^{\infty} W_{12max} \exp\left(-\frac{(t-nT)^2}{2\delta t_1^2}\right) \quad (14)$$

and

$$W_{21}(t) = \sum_{n=-\infty}^{\infty} W_{21max} \exp\left(-\frac{[t-(n+1/2)T]^2}{2\delta t_2^2}\right), \quad (15)$$

where

$$\begin{aligned}
 W_{12max} &= \frac{\sqrt{|V''_{xx}(x_1(t'),t')V''_{xx}(x_s(t'),t')|}}{2\pi} \\
 &\times \exp\left[\frac{V(x_1(t'),t') - V(x_s(t'),t')}{D}\right], \\
 t' &= 0, \\
 W_{21max} &= \frac{\sqrt{|V''_{xx}(x_2(t'),t')V''_{xx}(x_s(t'),t')|}}{2\pi} \\
 &\times \exp\left[\frac{V(x_2(t'),t') - V(x_s(t'),t')}{D}\right], \\
 t' &= \frac{T}{2}.
 \end{aligned} \tag{16}$$

The time independent transition rates  $W_{12max}$  and  $W_{21max}$  represent the maximum values that  $W_{12}$  and  $W_{21}$  attain during the period  $T$ . The fact that the rates  $W_{12}$  and  $W_{21}$  are effectively zero over half of the forcing period [due to condition (9)] means Eq. (7) simplifies as follows:

$$\dot{w}_1 = \begin{cases} -W_{12}w_1 & -T/4 < \tau < T/4, \\ W_{21}w_2 & T/4 < \tau < 3T/4, \end{cases} \tag{17a}$$

$$\dot{w}_2 = \begin{cases} W_{12}w_1 & -T/4 < \tau < T/4, \\ -W_{21}w_2 & T/4 < \tau < 3T/4, \end{cases} \tag{17b}$$

$$w_1 + w_2 = 1, \tag{17c}$$

$$\tau = -T/4 + [(t + T/4) \bmod T]. \tag{17d}$$

### III. SWITCHING TIME DISTRIBUTIONS AND THE STATISTICS ASSOCIATED WITH THEM

#### A. The residence time distribution

We first proceed to calculate the residence time distribution. In the following section, this calculation is generalized to obtain the return time density as well as the higher order switching time distributions. Before proceeding with the calculation, we discuss the influence that condition (9) has on the switching time dynamics. In this regime, the dynamics of the transition process are considerably simplified. To understand why, consider Fig. 1(a) that plots the time dependent transition rates  $W_{12}$  and  $W_{21}$  over an interval of  $\frac{5}{2}T$ . Each peak is approximately Gaussian with standard deviation  $\delta t_1$  (for the  $W_{12}$  peaks) given by Eq. (11) and  $\delta t_2$  (for the  $W_{21}$  peaks) given by (13). When condition (9) is satisfied  $\delta t_1, \delta t_2 \ll T$  and, thus, the transition probabilities are highly localized about integer multiples of  $T/2$ . As illustrated in Fig. 1(b), this means that transitions from the state 1 to 2 can only occur near (but not precisely at) times  $nT$ , and the transitions from the state 2 to 1 can only occur near times  $(n + 1/2)T$ . The net effect of this is that only a maximum of one transi-

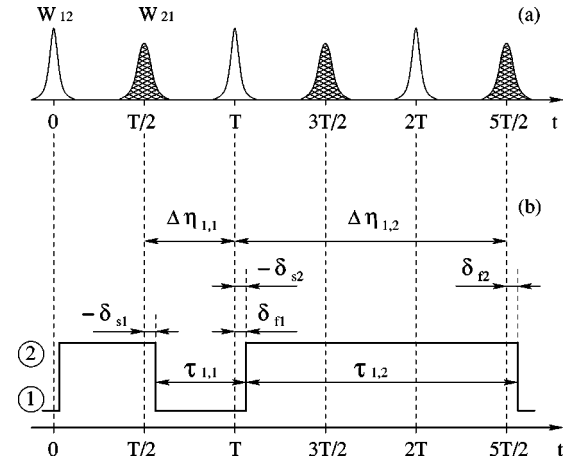


FIG. 1. (a) The transition rates  $W_{12}(t)$  and  $W_{21}(t)$  and (b) typical response of the two-state filter.

tion can occur every half cycle, thus placing a lower bound (of approximately  $T/2$ ) on the (residence) time that the system can remain in each state.

As we will see, the above considerations will enable us to develop a method for calculating the switching time distributions based on a decomposition of the transition sequence into a sum of independent random variables. This technique, developed for the symmetric system [14], differs from previous theoretical approaches [8,9,20] and has a number of advantage; for example, the switching time dynamics of the whole hierarchy of switching time distributions can be obtained and the variation in the phase at the switching point (phase distribution) is easily taken into account.

First, we need to introduce some notation. We denote by  $\tau_{j,l}$  the time between  $j + 1$  ( $j = 1, 2, \dots$ ) transitions when the first transition was to state  $l$  [where  $l \in (1, 2)$ ]. With this definition  $\tau_{1,1}$  denotes the time between two transitions when the first transition was to state 1 and  $\tau_{1,2}$  denotes the time between two transitions when the first transition was to state 2. These intervals are shown in Fig. 1(b). Clearly, this is a rather complicated way of saying that  $\tau_{1,1}$  and  $\tau_{1,2}$  are the residence times of state 1 and 2, respectively. However, this definition is required when we calculate the distribution of return times and higher order switching distributions. The residence times can now be decomposed into a sum of three independent random variables [see Fig. 1(b)]

$$\tau_{1,1} = \Delta \eta_{1,1} + \delta_{s1} + \delta_{f1},$$

$$\tau_{1,2} = \Delta \eta_{1,2} + \delta_{s2} + \delta_{f2}.$$

The variables  $\Delta \eta_{1,1}$  and  $\Delta \eta_{1,2}$  carry the periodic information and can only take on values of  $(m + 1/2)T$ ,  $m = 0, 1, 2, \dots$ . The variables  $\delta_{s1}$ ,  $\delta_{f1}$ ,  $\delta_{s2}$ , and  $\delta_{f2}$  are continuous and take on values  $[-T/4; T/4]$ . These variables take into account the smearing of the transition point due to noise, i.e., they allow for the fact that the transitions do not occur precisely at integer multiples of  $T/2$ . The variable  $\delta_{s1}$  takes into account the smearing when the system makes a transition from state 2 to state 1 ( $s$  denotes that this is the start of the transition sequence) and  $\delta_{f1}$  takes into account the

smearing when the system makes a transition from state 1 to state 2 ( $f$  denotes that this is the end of the transition sequence). The variables  $\delta_{s2}$  and  $\delta_{f2}$  are the same but for the opposite transition sequence, i.e., the start of the sequence is the transition from state 1 to 2 and the end of the sequence is the transition from state 2 to 1. Clearly,  $\delta_{s1}$  and  $-\delta_{f2}$  have identical distributions (i.e., they are independent identically distributed) as are  $\delta_{s2}$  and  $-\delta_{f1}$ .

We may now proceed with the calculation of the residence time distributions. Our method is based on the calculation of the characteristic functions  $C_{1,1}$  and  $C_{1,2}$  of the random variables  $\tau_{1,1}$  and  $\tau_{1,2}$ , respectively. These characteristic function are related to the residence time distributions  $P_{1,l}$  where  $l \in (1,2)$ , through the Fourier transform,

$$C_{1,l}(\omega) = \int_0^\infty P_{1,l}(\tau_{1,l}) \exp(i\omega\tau_{1,l}) d\tau_{1,l}, \quad (18)$$

with the inverse Fourier transform giving  $P_{1,l}(\tau_{1,l})$ ,

$$P_{1,l}(\tau_{1,l}) = \frac{1}{2\pi} \int_{-\infty}^\infty C_{1,l}(\omega) \exp(i\omega\tau_{1,l}) d\omega. \quad (19)$$

It is easy to see that the characteristic functions are the average of the exponential functions

$$C_{1,1}(\omega) = \langle \exp(i\omega\tau_{1,1}) \rangle,$$

$$C_{1,2}(\omega) = \langle \exp(i\omega\tau_{1,2}) \rangle.$$

Since the residence times include a sum of three independent random variables, the characteristic functions can be rewritten as

$$\begin{aligned} C_{1,1}(\omega) &= \langle \exp[i\omega(\Delta\eta_{1,1} + \delta_{s1} + \delta_{f1})] \rangle \\ &= \langle \exp(i\omega\Delta\eta_{1,1}) \rangle \langle \exp(i\omega\delta_{s1}) \rangle \langle \exp(i\omega\delta_{f1}) \rangle \\ &= C_{\Delta\eta_{1,1}}(\omega) C_{\delta_{s1}}(\omega) C_{\delta_{f1}}(\omega). \end{aligned} \quad (20)$$

Similarly,

$$\begin{aligned} C_{1,2}(\omega) &= \langle \exp[i\omega(\Delta\eta_{1,2} + \delta_{s2} + \delta_{f2})] \rangle \\ &= \langle \exp(i\omega\Delta\eta_{1,2}) \rangle \langle \exp(i\omega\delta_{s2}) \rangle \langle \exp(i\omega\delta_{f2}) \rangle \\ &= C_{\Delta\eta_{1,2}}(\omega) C_{\delta_{s2}}(\omega) C_{\delta_{f2}}(\omega). \end{aligned} \quad (21)$$

Clearly, the problem has been reduced to the calculation of the characteristic functions  $C_{\Delta\eta_{1,1}}(\omega)$ ,  $C_{\Delta\eta_{1,2}}(\omega)$ ,  $C_{\delta_{s1}}(\omega)$ ,  $C_{\delta_{s2}}(\omega)$ , and  $C_{\delta_{f2}}(\omega)$ .

The characteristic function  $C_{\Delta\eta_{1,1}}(\omega)$  can be found by first calculating its associated distribution,  $P_{\Delta\eta_{1,1}}$ . To obtain this distribution we need to know the probability  $p$  that the system remains in state 1 for a complete cycle of the driving force. [consequently,  $(1-p)$  is the probability per period that the system will escape from state 1]. This probability can be obtained by considering the decay of the population of state 1 over a complete forcing cycle. The equation governing the population is

$$\dot{w}_1 = -W_{12}(t)w_1, \quad (22)$$

with the initial condition  $w_1(t_1) = 1$ . This can be formally integrated to yield

$$w_1(t) = \exp\left(-\int_{t_1}^t W_{12}(s) ds\right). \quad (23)$$

The probability to remain in state 1 for one period  $T$  is then given by  $w_1(t_1+T)$ . Using Eq. (14), we can write

$$\begin{aligned} w_1(t_1+T) &= \exp\left(-\int_{t_1}^{t_1+T} W_{12}(s) ds\right) \\ &= \exp\left(-\int_{-T/4}^{T/4} W_{12max} \exp\left[-\frac{t^2}{2\delta t_1^2}\right] dt\right) \\ &\approx \exp(-\sqrt{2\pi} W_{12max} \delta t_1) = \exp(-I_1) = p, \end{aligned} \quad (24)$$

where we have defined

$$I_1 = \int_{-T/4}^{T/4} W_{12}(t) dt \approx \sqrt{2\pi} W_{12max} \delta t_1. \quad (25)$$

The probability to switch from state 1 to 2 in the first period is therefore  $(1-p)$  and in this case, we have (Fig. 1)  $\Delta\eta_{1,1} = T/2$ . However, if the system switches during the second period then we have  $\Delta\eta_{1,1} = 3T/2$  and this will occur with probability  $(1-p)p$ . In general, if the system switches during the  $(m+1)$ th period then  $\Delta\eta_{1,1} = (m+1/2)T$  and this will occur with probability  $(1-p)p^m$ . It is easy to see therefore that the probability density function  $P_{\Delta\eta_{1,1}}(\Delta\eta_{1,1})$  is given by

$$P_{\Delta\eta_{1,1}}(\Delta\eta_{1,1}) = \sum_{m=0}^{\infty} (1-p)p^m \delta(\Delta\eta_{1,1} - (m+1/2)T). \quad (26)$$

The characteristic function can be found by taking the Fourier transform

$$\begin{aligned} C_{\Delta\eta_{1,1}}(\omega) &= \int_0^\infty P_{\Delta\eta_{1,1}}(\Delta\eta_{1,1}) \exp(i\omega\Delta\eta_{1,1}) d\Delta\eta_{1,1} \\ &= (1-p) \exp(i\omega T/2) \sum_{m=0}^{\infty} [p \exp(i\omega T)]^m \\ &= \frac{1}{\cos(\omega T/2) - i\alpha_p \sin(\omega T/2)}, \end{aligned} \quad (27)$$

where  $\alpha_p = (1+p)/(1-p)$ .

To find the distribution  $P_{\delta_{f1}}(\delta_{f1})$ —which is the distribution of switching times around times  $mT$ —we need to again consider the solution of Eq. (22) over a single forcing period. Due to condition (9),  $W_{12}$  is effectively zero outside the range  $[-T/4; T/4]$  and hence, we can write

$$w_1(\delta_{f1}) = C_0 \exp\left(-\int_{-T/4}^{\delta_{f1}} W_{12}(s) ds\right), \quad (28)$$

which is interpreted as the probability of remaining in state 1 for the time interval  $(\delta_{f1} + T/4)$ . The probability to escape from the state 1 is therefore  $[1 - w_1(\delta_{f1})]$ . The probability density of  $\delta_{f1}$  is now given by

$$\begin{aligned} P_{\delta_{f1}}(\delta_{f1}) &= \frac{d}{d\delta_{f1}} [1 - w_1(\delta_{f1})] \\ &= C_0 W_{12}(\delta_{f1}) \exp\left(-\int_{-T/4}^{\delta_{f1}} W_{12}(s) ds\right), \end{aligned} \quad (29)$$

where the normalization constant  $C_0$  can be found from the condition

$$1 = \int_{-T/4}^{T/4} P_{\delta_{f1}}(\delta_{f1}) d\delta_{f1} = C_0(1-p),$$

which yields  $C_0 = (1-p)^{-1}$ . To a good degree of approximation (see Appendix) Eq. (29) can be approximated as a Gaussian with mean  $\delta_{f1m}$  and standard deviation  $\sigma_{f1}$ , i.e.,

$$P_{\delta_{f1}}(\delta_{f1}) = \frac{1}{\sqrt{2\pi\sigma_{f1}^2}} \exp\left(-\frac{(\delta_{f1} - \delta_{f1m})^2}{2\sigma_{f1}^2}\right). \quad (30)$$

It is worth pointing out that, in general,  $\delta_{f1}$  has a nonzero mean value that is always negative. This implies that, on an average, transitions occur *before* the maximum in  $W_{12}$ . The exact amount of the shift depends on the forcing frequency (see Appendix for details).

The characteristic function  $C_{\delta_{f1}}(\omega)$  can now easily be obtained from Eq. (30) as

$$\begin{aligned} C_{\delta_{f1}}(\omega) &= \int_{-\infty}^{\infty} P_{\delta_{f1}}(\delta_{f1}) \exp(i\omega\delta_{f1}) d\delta_{f1} \\ &= \exp(i\omega\delta_{f1m}) \exp\left(-\frac{\omega^2\sigma_{f1}^2}{2}\right). \end{aligned} \quad (31)$$

By considering the switching dynamics from state 2, exactly the same procedures can be employed to obtain the remaining characteristic functions  $C_{\Delta\eta_{1,2}}(\omega)$ ,  $C_{\delta_{s1}}(\omega)$ ,  $C_{\delta_{f2}}(\omega)$ , and  $C_{\delta_{s2}}$ . We obtain

$$P_{\Delta\eta_{1,2}}(\Delta\eta_{1,2}) = \sum_{m=0}^{\infty} (1-q)q^m \delta(\Delta\eta_{1,2} - (m+1/2)T), \quad (32)$$

where  $q$  is the probability of remaining in state 2 for one period  $T$ :

$$q = \exp(-I_2), \quad (33)$$

with

$$I_2 = \int_{T/4}^{3T/4} W_{21}(t) dt \approx \sqrt{2\pi} W_{21max} \delta t_2. \quad (34)$$

Therefore,

$$\begin{aligned} C_{\Delta\eta_{1,2}}(\omega) &= \int_0^{\infty} P_{\Delta\eta_{1,2}}(\Delta\eta_{1,2}) \exp(i\omega\Delta\eta_{1,2}) d\Delta\eta_{1,2} \\ &= (1-q) \exp(i\omega T/2) \sum_{m=0}^{\infty} [q \exp(i\omega T)]^m \\ &= \frac{1}{\cos(\omega T/2) - i\alpha_q \sin(\omega T/2)}, \end{aligned} \quad (35)$$

where  $\alpha_q = (1+q)/(1-q)$ , and

$$P_{\delta_{f2}}(\delta_{f2}) = P_{\delta_{f2}}(\delta_{f2}) \exp\left(-\frac{(\delta_{f2} - \delta_{f2m})^2}{2\sigma_{f2}^2}\right). \quad (36)$$

The remaining characteristic functions can be obtained by noting that

$$P_{\delta_{f1}}(\delta_{f1}) = P_{\delta_{s2}}(-\delta_{f1})$$

and

$$P_{\delta_{f2}}(\delta_{f2}) = P_{\delta_{s1}}(-\delta_{f2}),$$

i.e., the average values  $\delta_{f2m} = -\delta_{s1m}$  and  $\delta_{f1m} = -\delta_{s2m}$ . This implies that the characteristic functions of  $\delta_{s1}$  and  $\delta_{s2}$  are the complex conjugate of the characteristic functions for  $\delta_{f2}$  and  $\delta_{f1}$ :

$$C_{\delta_{s1}}(\omega) = C_{\delta_{f2}}^*(\omega), \quad C_{\delta_{s2}}(\omega) = C_{\delta_{f1}}^*(\omega).$$

Having obtained all the necessary characteristic functions, the residence time distributions can finally be calculated from Eqs. (20) and (21) as

$$\begin{aligned} P_{1,1}(\tau_{1,1}) &= \frac{1-p}{\sqrt{2\pi(\sigma_{s1}^2 + \sigma_{f1}^2)}} \sum_{m=0}^{\infty} p^m \\ &\times \exp\left(-\frac{[\tau_{1,1} - (m+1/2)T - \delta_{s1m} - \delta_{f1m}]^2}{2(\sigma_{s1}^2 + \sigma_{f1}^2)}\right) \end{aligned} \quad (37)$$

and

$$\begin{aligned} P_{1,2}(\tau_{1,2}) &= \frac{1-q}{\sqrt{2\pi(\sigma_{s2}^2 + \sigma_{f2}^2)}} \sum_{m=0}^{\infty} q^m \\ &\times \exp\left(-\frac{[\tau_{1,2} - (m+1/2)T - \delta_{s2m} - \delta_{f2m}]^2}{2(\sigma_{s2}^2 + \sigma_{f2}^2)}\right). \end{aligned} \quad (38)$$

### The average residence times

Having obtained the residence time distributions, it is now straightforward to find the average residence times themselves. The residence times are given by the first moments of the distributions  $P_{1,1}(\tau_{1,1})$  and  $P_{1,2}(\tau_{1,2})$

$$\begin{aligned}\langle \tau_{1,1} \rangle &= \int_0^\infty \tau_{1,1} P_{1,1}(\tau_{1,1}) d\tau_{1,1} \\ &= (1-p) \sum_{m=0}^{\infty} p^m [(m+1/2)T + \delta_{s1m} + \delta_{f1m}] \\ &= \alpha_p \frac{T}{2} + \delta_{s1m} + \delta_{f1m}\end{aligned}\quad (39)$$

and

$$\begin{aligned}\langle \tau_{1,2} \rangle &= \int_0^\infty \tau_{1,2} P_{1,2}(\tau_{1,2}) d\tau_{1,2} \\ &= (1-q) \sum_{m=0}^{\infty} q^m [(m+1/2)T + \delta_{s2m} + \delta_{f2m}] \\ &= \alpha_q \frac{T}{2} + \delta_{s2m} + \delta_{f2m}.\end{aligned}\quad (40)$$

The difference between the first moments,  $\Delta T$ , can also be easily calculated (noting  $\delta_{s1m} = -\delta_{f2m}$  and  $\delta_{f1m} = -\delta_{s2m}$ ) to be

$$\begin{aligned}\Delta T = \langle \tau_{1,1} \rangle - \langle \tau_{1,2} \rangle &= [\alpha_p - \alpha_q] \frac{T}{2} + \delta_{s1m} + \delta_{f1m} - \delta_{s2m} - \delta_{f2m} \\ &= [\alpha_p - \alpha_q] \frac{T}{2} + 2(\delta_{s1m} + \delta_{f1m}).\end{aligned}\quad (41)$$

These expressions can be simplified further under the condition that the system is almost synchronized to the driving field. In this situation, the system is switching every half period and hence  $\alpha_p = \alpha_q = 1$  (since  $p = q = 0$ ). Hence, the residence times reduce to  $\langle \tau_{1,1} \rangle = \delta_{s1m} + \delta_{f1m}$  and  $\langle \tau_{1,2} \rangle = \delta_{s2m} + \delta_{f2m}$ , and  $\Delta T = 2(\delta_{s1m} + \delta_{f1m})$ .

For the case  $|c| \ll D \ll \Delta V$  (where  $\Delta V = \min\{|V(x_1, t) - V(x_s, t)|, |V(x_2, t) - V(x_s, t)|\}$ ), an approximate expression for the dependence of  $\Delta T$  on the asymmetry can be found. In this situation, the probability  $p$  and  $q$  can be approximated as

$$\begin{aligned}p &= \exp(-I_1) = \sum_{n=0}^{\infty} (-I_1)^n / n! \approx 1 - I_1, \\ q &= \exp(-I_2) = \sum_{n=0}^{\infty} (-I_2)^n / n! \approx 1 - I_2,\end{aligned}$$

where it is assumed  $I_{1,2} \ll 1$ .

The parameters  $\delta_{s1m}$  and  $\delta_{f1m}$  can be found as  $\delta_{f1m} = -I_1 \delta t_1 / \sqrt{2\pi}$  and  $\delta_{s1m} = I_2 \delta t_2 / \sqrt{2\pi}$  in the limit of weak noise intensity (see Appendix). The residence times can, therefore, be approximated as

$$\langle \tau_{1,1} \rangle = \frac{T}{I_1} + \frac{I_2 \delta t_2 - I_1 \delta t_1}{\sqrt{2\pi}} \quad (42)$$

and

$$\langle \tau_{1,2} \rangle = \frac{T}{I_2} + \frac{I_1 \delta t_1 - I_2 \delta t_2}{\sqrt{2\pi}}, \quad (43)$$

and the difference between the average residence times is

$$\Delta T \approx \frac{T}{I_1} - \frac{T}{I_2} + \frac{2(I_2 \delta t_2 - I_1 \delta t_1)}{\sqrt{2\pi}}.$$

Assuming  $\delta t_1 \approx \delta t_2 = \delta t$ , we can rewrite this last expression

$$\Delta T = \frac{T(I_2 - I_1)}{I_1 I_2} \left( 1 + 2I_1 I_2 \frac{\delta t}{T\sqrt{2\pi}} \right) \approx \frac{T(I_2 - I_1)}{I_1 I_2} = \frac{T}{I_1} - \frac{T}{I_2}, \quad (44)$$

where  $|2I_1 I_2 \delta t / T\sqrt{2\pi}| \ll 1$ .

Using Eqs. (25) and (34) and assuming the parameter  $c$  is sufficiently weak such that  $V''_{xx}(x_1, 0) \approx V''_{xx}(x_2, T/2)$ , and  $V''_{xx}(x_{s1}, 0) \approx V''_{xx}(x_{s2}, T/2)$ , where  $x_1 = x_1(0)$ ,  $x_{s1} = x_s(0)$ ,  $x_{s2} = x_s(T/2)$ , and  $x_2 = x_2(T/2)$ ,  $\Delta T$  can be rewritten as

$$\begin{aligned}\Delta T &= \frac{T}{\sqrt{2\pi} \delta t} \left( \frac{1}{W_{12max}} - \frac{1}{W_{21max}} \right) \\ &\approx \frac{T\sqrt{2\pi}}{\delta t \sqrt{|V''_{xx}(x_1, 0) V''_{xx}(x_{s1}, 0)|}} \\ &\quad \times \left[ \exp\left(\frac{\Delta U_{1s}}{D}\right) - \exp\left(\frac{\Delta U_{2s}}{D}\right) \right],\end{aligned}$$

where

$$\Delta V_{1s} = V(x_{s1}, 0) - V(x_1, 0) = \Delta U_{1s} + \Delta_{1s} c,$$

$$\Delta U_{1s} = V(x_{s1}, 0)_{c=0} - V(x_1, 0)_{c=0} = U(x_s, 0) - U(x_1, 0),$$

$$\Delta_{1s} = \left( \frac{dV(x_{s1}, 0)}{dc} - \frac{dV(x_1, 0)}{dc} \right)_{c=0} = (x_{s1} - x_1)_{c=0},$$

$$\Delta V_{2s} = V(x_2, T/2) - V(x_{s2}, T/2) = \Delta U_{2s} + \Delta_{2s} c,$$

$$\begin{aligned}\Delta U_{2s} &= V(x_2, T/2)_{c=0} - V(x_{s2}, T/2)_{c=0} \\ &= U(x_2, T/2) - U(x_{s2}, T/2) = \Delta U_{1s} = \Delta U,\end{aligned}$$

$$\begin{aligned}\Delta_{2s} &= \left( \frac{dV(x_2, T/2)}{dc} - \frac{dV(x_{s2}, T/2)}{dc} \right)_{c=0} \\ &= (x_2 - x_{s2})_{c=0} = -\Delta_{1s} = -\Delta_x.\end{aligned}$$

This yields

$$\begin{aligned}
 \Delta T &\approx \frac{T\sqrt{2\pi}}{\delta t \sqrt{|V''_{xx}(x_1,0)V''_{xx}(x_{s1},0)|}} \\
 &\times \exp\left(\frac{\Delta U}{D}\right) \left[ \exp\left(\frac{\Delta_x c}{D}\right) - \exp\left(\frac{-\Delta_x c}{D}\right) \right] \\
 &\approx \frac{T\sqrt{2\pi} \exp(\Delta U/D)}{\delta t \sqrt{|V''_{xx}(x_1,0)V''_{xx}(x_{s1},0)|}} \\
 &\times \left[ 1 + \frac{\Delta_x c}{D} + \frac{1}{2} \left(\frac{\Delta_x c}{D}\right)^2 - 1 + \frac{\Delta_x c}{D} - \frac{1}{2} \left(\frac{\Delta_x c}{D}\right)^2 \right] \\
 &\approx \frac{T\sqrt{2\pi}}{\delta t \sqrt{|V''_{xx}(x_1,0)V''_{xx}(x_{s1},0)|}} \exp\left(\frac{\Delta U}{D}\right) \frac{2\Delta_x c}{D}. \quad (45)
 \end{aligned}$$

Finally, noting that  $\delta t = \sqrt{D/\Delta_x A \Omega^2}$ , we obtain the final expression as

$$\begin{aligned}
 \Delta T &\approx 2(2\pi\Delta_x)^{3/2} \sqrt{\frac{A}{D|V''_{xx}(x_1,0)V''_{xx}(x_{s1},0)|}} \exp\left(\frac{\Delta U}{D}\right) \frac{c}{D} \\
 &+ O((c/D)^3). \quad (46)
 \end{aligned}$$

Note that the next correction is  $O((c/D)^3)$  and, hence, Eq. (46) is expected to be a good approximation over a wide range of  $c$ .

### B. The return time and higher order distributions

In the last section, we calculated the residence time distribution and the average residence times. This calculation will now be generalized to enable the return time and higher order switching time distributions to be obtained.

The next distribution in the hierarchy is the so called return time distribution [21]. This distribution is defined as the time required for the system to switch from one state to the other and then back again and, hence, it is the time between three switching events. In our notation, we write  $\tau_{2,1}$ —this is the time taken for the system to start in state 1 (the timing starts when the system first makes a transition to state 1), make a transition to state 2, and then return back to state 1. Similarly, we write  $\tau_{2,2}$  to represent the opposite sequence (i.e., start in state 2, switch to state 1, and then return to state 2). The probability density functions  $P_{2,1}(\tau_{2,1})$  and  $P_{2,2}(\tau_{2,2})$  associated with these times are referred to as the return time densities. We can continue this line of reasoning and define density functions for an arbitrary number of switching events as  $\tau_{j,1}$  and  $\tau_{j,2}$  where  $j = 1, 2, 3, \dots$ . For example,  $\tau_{4,1}$  would be the time required for the system, starting in state 1, to make the transition sequence  $1 \rightarrow 2, 2 \rightarrow 1, 1 \rightarrow 2$ , and finally,  $2 \rightarrow 1$ . Of most interest are the residence and return time distributions. However, in certain cases, such as in the calculation of the power spectral density of the system (see Ref. [7]), it is necessary to know the whole hierarchy of distributions.

We now consider the calculation of the hierarchy of switching time distributions with emphasis on the return time distribution. In a similar fashion to the residence times, the return times can be decomposed into a set of independent elemental switching events

$$\tau_{2,1} = \Delta \eta_{1,1} + \Delta \eta_{2,2} + \delta_{s1} + \delta_{f1},$$

$$\tau_{2,2} = \Delta \eta_{1,2} + \Delta \eta_{2,1} + \delta_{s2} + \delta_{f2},$$

where  $\Delta \eta_{2,2}$  is the length of the second time interval spent in state 2 and  $\Delta \eta_{2,1}$  is the length of the second time interval spent in state 1. We can extend this notation to denote the time interval between switching event  $k$  and  $(k+1)$  as  $\Delta \eta_{k,l}$ . The  $l \in (1,2)$  denotes which state the system was in between the two switching events. Therefore, for the general case, we have the following decomposition:

$$\begin{aligned}
 \tau_{j,1} &= \sum_{k=1}^j \Delta \eta_{k,[2-(k \bmod 2)]} + \delta_{s1} + \delta_{f[2-(j \bmod 2)]} \\
 &= \Delta \eta_{1,1} + \Delta \eta_{2,2} + \Delta \eta_{3,1} + \Delta \eta_{4,2} + \dots + \delta_{s1} \\
 &\quad + \delta_{f[2-(j \bmod 2)]},
 \end{aligned}$$

which starts from the state 1, and

$$\begin{aligned}
 \tau_{j,2} &= \sum_{k=1}^j \Delta \eta_{k,[1+(k \bmod 2)]} + \delta_{s2} + \delta_{f[1+(j \bmod 2)]} \\
 &= \Delta \eta_{1,2} + \Delta \eta_{2,1} + \Delta \eta_{3,2} + \Delta \eta_{4,1} + \dots + \delta_{s2} \\
 &\quad + \delta_{f[1+(j \bmod 2)]},
 \end{aligned}$$

which starts from the state 2.

As before, we calculate the return time densities via the characteristic functions:

$$C_{2,1}(\omega) = \int_0^\infty \exp(i\omega \tau_{2,1}) P_{2,1}(\tau_{2,1}) d\tau_{2,1},$$

$$C_{2,2}(\omega) = \int_0^\infty \exp(i\omega \tau_{2,2}) P_{2,2}(\tau_{2,2}) d\tau_{2,2}.$$

These can be broken down into a product of elemental characteristic functions as follows,

$$\begin{aligned}
 C_{2,1}(\omega) &= \langle \exp[i\omega(\Delta \eta_{1,1} + \Delta \eta_{2,2} + \delta_{s1} + \delta_{f2})] \rangle \\
 &= \langle \exp(i\omega \Delta \eta_{1,1}) \rangle \langle \exp(i\omega \Delta \eta_{2,2}) \rangle \langle \exp(i\omega \delta_{s1}) \rangle \\
 &\quad \times \langle \exp(i\omega \delta_{f2}) \rangle \\
 &= C_{\Delta \eta_{1,1}}(\omega) C_{\Delta \eta_{2,2}}(\omega) C_{\delta_{s1}}(\omega) C_{\delta_{f2}}(\omega),
 \end{aligned}$$

$$\begin{aligned}
 C_{2,2}(\omega) &= \langle \exp[i\omega(\Delta \eta_{1,2} + \Delta \eta_{2,1} + \delta_{s2} + \delta_{f1})] \rangle \\
 &= \langle \exp(i\omega \Delta \eta_{1,2}) \rangle \langle \exp(i\omega \Delta \eta_{2,1}) \rangle \langle \exp(i\omega \delta_{s2}) \rangle \\
 &\quad \times \langle \exp(i\omega \delta_{f1}) \rangle \\
 &= C_{\Delta \eta_{1,2}}(\omega) C_{\Delta \eta_{2,1}}(\omega) C_{\delta_{s2}}(\omega) C_{\delta_{f1}}(\omega).
 \end{aligned}$$

The only characteristic functions that were not calculated in the last section are  $C_{\Delta\eta_{2,2}}(\omega)$  and  $C_{\Delta\eta_{2,1}}(\omega)$ . However, these can trivially be obtained by noting that the variables  $\Delta\eta_{2,2}$  and  $\Delta\eta_{1,2}$  are identically distributed and hence  $C_{\Delta\eta_{2,2}}(\omega) = C_{\Delta\eta_{1,2}}(\omega)$ , where  $C_{\Delta\eta_{1,2}}(\omega)$  is given in Eq. (35). Similarly,  $C_{\Delta\eta_{2,1}}(\omega) = C_{\Delta\eta_{1,1}}(\omega)$ , where  $C_{\Delta\eta_{1,1}}(\omega)$  is given in Eq. (27). By noting that  $\sigma_{s1}^2 = \sigma_{f2}^2$  and  $\sigma_{s2}^2 = \sigma_{f1}^2$ , the inverse Fourier transform of  $C_{2,1}(\omega)$  and  $C_{2,2}(\omega)$  can now be taken to obtain the return time densities,

$$P_{2,1}(\tau_{2,1}) = (1-p)(1-q) \sum_{n=0}^{\infty} p^n \sum_{m=0}^{\infty} q^m \frac{1}{\sqrt{4\pi\sigma_{s1}^2}} \times \exp\left(-\frac{[\tau_{2,1} - (m+n)T]^2}{4\sigma_{s1}^2}\right) \quad (47)$$

and

$$P_{2,2}(\tau_{2,2}) = (1-p)(1-q) \sum_{n=0}^{\infty} p^n \sum_{m=0}^{\infty} q^m \frac{1}{\sqrt{4\pi\sigma_{s2}^2}} \times \exp\left(-\frac{[\tau_{2,2} - (m+n)T]^2}{4\sigma_{s2}^2}\right). \quad (48)$$

The generalized expressions for the probability densities  $P_{j,1}(\tau_{j,1})$  and  $P_{j,2}(\tau_{j,2})$  can be found in a similar fashion. We consider the cases of odd and even  $j$  separately. Taking  $j$  odd and noting that all variables  $\Delta\eta_{k,1}$  are identically distributed, as are all the variables  $\Delta\eta_{k,2}$ , we can write

$$\tau_{2r+1,1} = \sum_{l=0}^r \Delta\eta_{2l+1,1} + \sum_{l=1}^r \Delta\eta_{2l,2} + \delta_{s1} + \delta_{f1}$$

and

$$\tau_{2r+1,2} = \sum_{l=0}^r \Delta\eta_{2l+1,2} + \sum_{l=1}^r \Delta\eta_{2l,1} + \delta_{s2} + \delta_{f2},$$

where  $r=1,2,3,\dots$ . The characteristic function for state 1 can now be written as

$$C_{2r+1,1}(\omega) = \left(\prod_{n=0}^r C_{\Delta\eta_{2n+1,1}}(\omega)\right) \times \left(\prod_{m=1}^r C_{\Delta\eta_{2m,2}}(\omega)\right) C_{\delta_{s1}}(\omega) C_{\delta_{f1}}(\omega) = C_{\Delta\eta_{1,1}}^{r+1}(\omega) C_{\Delta\eta_{1,2}}^r(\omega) C_{\delta_{s1}}(\omega) C_{\delta_{f1}}(\omega),$$

which can be rewritten as

$$C_{2r+1,1}(\omega) = (1-p)^{r+1}(1-q)^r \exp\{i\omega[(r+1/2)T + \delta_{s1m} + \delta_{f1m}]\} \exp[-\omega^2(\sigma_{s1}^2 + \sigma_{f1}^2)/2] \times \left(\sum_{n=0}^{\infty} \exp(i\omega nT - nI_1)\right)^{r+1} \times \left(\sum_{m=0}^{\infty} \exp(i\omega mT - mI_2)\right)^r$$

or

$$C_{2r+1,1}(\omega) = (1-p)^{r+1}(1-q)^r \exp\{i\omega[(r+1/2)T + \delta_{s1m} + \delta_{f1m}]\} \exp[-\omega^2(\sigma_{s1}^2 + \sigma_{f1}^2)/2] \times \sum_{n_1, n_2, \dots, n_{r+1}=0}^{\infty} \exp[(n_1 + n_2 + \dots + n_{r+1})(i\omega T - I_1)] \sum_{m_1, m_2, \dots, m_r=0}^{\infty} \exp[(m_1 + m_2 + \dots + m_r)(i\omega T - I_2)].$$

A change of variables to  $n = n_1 + n_2 + \dots + n_{r+1}$  and  $m = m_1 + m_2 + \dots + m_r$  can now be performed to give

$$C_{2r+1,1}(\omega) = (1-p)^{r+1}(1-q)^r \exp\{i\omega[(r+1/2)T + \delta_{s1m} + \delta_{f1m}]\} \exp[-\omega^2(\sigma_{s1}^2 + \sigma_{f1}^2)/2] \times \sum_{n=0}^{\infty} \frac{(r+n)!}{r!n!} \exp[n(i\omega T - I_1)] \times \sum_{m=0}^{\infty} \frac{(r+m-1)!}{(r-1)!m!} \exp[m(i\omega T - I_2)].$$

Taking the inverse Fourier transform gives

$$P_{2r+1,1}(\tau_{2r+1,1}) = (1-p)^{r+1}(1-q)^r \sum_{n=0}^{\infty} \frac{(r+n)!}{r!n!} p^n \times \sum_{m=0}^{\infty} \frac{(r+m-1)!}{(r-1)!m!} q^m \frac{1}{2\pi} \times \int_{-\infty}^{\infty} \exp\{i\omega[(r+m+n+1/2)T + \delta_{s1m} + \delta_{f1m} - \tau_{2r+1,1}]\} \exp\left(-\frac{\omega^2}{2}(\sigma_{s1}^2 + \sigma_{f1}^2)\right) d\omega,$$

and the final expression is

$$P_{2r+1,1}(\tau_{2r+1,1}) = (1-p)^{r+1}(1-q)^r \sum_{n=0}^{\infty} \frac{(r+n)!}{r!n!} p^n \sum_{m=0}^{\infty} \frac{(r+m-1)!}{(r-1)!m!} q^m \frac{1}{\sqrt{2\pi(\sigma_{s1}^2 + \sigma_{f1}^2)}} \times \exp\left(-\frac{[(r+m+n+1/2)T + \delta_{s1m} + \delta_{f1m} - \tau_{2r+1,1}]^2}{2(\sigma_{s1}^2 + \sigma_{f1}^2)}\right). \tag{49}$$

Exactly the same procedure can be carried out for state 2 to obtain

$$P_{2r+1,2}(\tau_{2r+1,2}) = (1-p)^r(1-q)^{r+1} \sum_{n=0}^{\infty} \frac{(r+n-1)!}{(r-1)!n!} p^n \sum_{m=0}^{\infty} \frac{(r+m)!}{r!m!} q^m \frac{1}{\sqrt{2\pi(\sigma_{s2}^2 + \sigma_{f2}^2)}} \times \exp\left(-\frac{[(r+m+n+1/2)T + \delta_{s2m} + \delta_{f2m} - \tau_{2r+1,2}]^2}{2(\sigma_{s2}^2 + \sigma_{f2}^2)}\right). \tag{50}$$

The same methods can be applied to obtain the distributions for even  $j$ . The final results are

$$P_{2r,1}(\tau_{2r,1}) = (1-p)^r(1-q)^r \sum_{n=0}^{\infty} \frac{(r+n-1)!}{(r-1)!n!} p^n \times \sum_{m=0}^{\infty} \frac{(r+m-1)!}{(r-1)!m!} q^m \frac{1}{\sqrt{4\pi\sigma_{s1}^2}} \times \exp\left(-\frac{[(r+m+n)T - \tau_{2r,1}]^2}{4\sigma_{s1}^2}\right) \tag{51}$$

and

$$P_{2r,2}(\tau_{2r,2}) = (1-p)^r(1-q)^r \sum_{n=0}^{\infty} \frac{(r+n-1)!}{(r-1)!n!} p^n \times \sum_{m=0}^{\infty} \frac{(r+m-1)!}{(r-1)!m!} q^m \frac{1}{\sqrt{4\pi\sigma_{s2}^2}} \times \exp\left(-\frac{[(r+m+n)T - \tau_{2r,2}]^2}{4\sigma_{s2}^2}\right). \tag{52}$$

**1. The average return times**

The average return times are the first moments of the return time densities. They are defined as

$$\langle \tau_{2,1} \rangle = \int_0^{\infty} \tau_{2,1} P_{2,1}(\tau_{2,1}) d\tau_{2,1}$$

and

$$\langle \tau_{2,2} \rangle = \int_0^{\infty} \tau_{2,2} P_{2,2}(\tau_{2,2}) d\tau_{2,2}.$$

These times are identical and independent of the time shifts  $\delta_{s1m}$  and  $\delta_{f1m}$ :

$$\langle \tau_{2,1} \rangle = \langle \tau_{2,2} \rangle = (\alpha_p + \alpha_q) \frac{T}{2} = \langle T_R \rangle. \tag{53}$$

We will now obtain two approximations for  $\langle T_R \rangle$ , one valid for  $|c/D| \ll 1$  and the other for  $|c/D| \gg 1$ . The return time is the summation of the resident times  $\langle \tau_{1,1} \rangle$  and  $\langle \tau_{1,2} \rangle$ , and for weak noise can be approximated by expressions (42) and (43):

$$\langle T_R \rangle \approx \frac{T}{I_1} + \frac{T}{I_2}.$$

For  $|c/D| \ll 1$ , we can use Eqs. (25) and (34) to write the expression as

$$\langle T_R \rangle \approx \frac{T\sqrt{2\pi}}{\delta t \sqrt{|V''_{xx}(x_1,0)V''_{xx}(x_{s1},0)|}} \exp\left(\frac{\Delta U}{D}\right) \left[2 + \left(\frac{\Delta_x c}{D}\right)^2\right]. \tag{54}$$

This is the final expression valid for  $|c/D| \ll 1$ . Note, that in contrast to the residence time, in this limit the return time depends quadratically on  $c$ .

We now obtain an approximation valid for  $|c/D| \gg 1$ . In this case, the ratio of the residence times  $\langle \tau_{1,1} \rangle$  to  $\langle \tau_{1,2} \rangle$  is proportional to  $\exp(2c/D)$ . Consequently, for  $c > 0$ , we have  $\langle \tau_{1,1} \rangle \gg \langle \tau_{1,2} \rangle$  and hence, to a very good approximation,  $\langle T_R \rangle \approx \langle \tau_{1,1} \rangle$ . For  $c < 0$ , the situation is reversed and  $\langle T_R \rangle \approx \langle \tau_{1,2} \rangle$ . Therefore, for  $c > 0$ , we can write

$$\langle T_{R+} \rangle \approx \langle \tau_{1,1} \rangle = \frac{T}{\sqrt{2\pi} W_{12max} \delta t_1} = \frac{(2\pi)^{3/2} \sqrt{A|x_1 - x_s|}}{\sqrt{D|V''_{xx}(x_1,0)V''_{xx}(x_s,0)|}} \exp\left(\frac{\Delta V_{1s}}{D}\right),$$

where

$$\begin{aligned} \Delta V_{1s} &= V(x_s,0) - V(x_1,0) \\ &= -\frac{a}{2}(x_s^2 - x_1^2) + \frac{b}{4}(x_s^4 - x_1^4) - A(x_s - x_1) + c(x_s - x_1) \\ &= \Delta U_{1s} + c(x_s - x_1), \end{aligned}$$

and  $x_1 = x_1(0)$  and  $x_s = x_s(0)$ . Finally, this gives the approximation

$$\langle T_{R+} \rangle \approx \langle \tau_{1,1} \rangle = \frac{(2\pi)^{3/2} \sqrt{A|x_1 - x_s|}}{\sqrt{D|V''_{xx}(x_1,0)V''_{xx}(x_s,0)|}} \exp\left(\frac{\Delta U_{1s}}{D}\right) \times \exp\left(\frac{c}{D}(x_s - x_1)\right). \quad (55)$$

For  $c < 0$ , the average return time can be found in a similar manner.

$$\begin{aligned} \langle T_{R-} \rangle &\approx \langle \tau_{1,2} \rangle \approx \frac{T}{\sqrt{2\pi}W_{21max}\delta t_1} \\ &= \frac{(2\pi)^{3/2} \sqrt{A|x_2 - x_s|}}{\sqrt{D|V''_{xx}(x_2,T/2)V''_{xx}(x_s,T/2)|}} \exp\left(\frac{\Delta V_{1s}}{D}\right), \end{aligned}$$

$$\Delta V_{2s} = V(x_s, T/2) - V(x_2, T/2)$$

$$\begin{aligned} &= -\frac{a}{2}(x_s^2 - x_2^2) + \frac{b}{4}(x_s^4 - x_2^4) - A(x_s - x_2) + c(x_s - x_2) \\ &= \Delta U_{2s} + c(x_s - x_2), \end{aligned}$$

where  $x_2 = x_2(T/2)$  and  $x_s = x_s(T/2)$ . Finally,

$$\langle T_{R-} \rangle \approx \langle \tau_{1,2} \rangle = \frac{(2\pi)^{3/2} \sqrt{A|x_2 - x_s|}}{\sqrt{D|V''_{xx}(x_2,T/2)V''_{xx}(x_s,T/2)|}} \exp\left(\frac{\Delta U_{2s}}{D}\right) \times \exp\left(\frac{c}{D}(x_s - x_2)\right). \quad (56)$$

It should be noted that expressions (55) and (56) not only provide approximations to the average return time but also to the average residence times for  $|c/D| \gg 1$ . Clearly, all these expressions depend exponentially on  $c/D$ . This implies that even for  $c \ll 1$  (weak asymmetry), the affect of the asymmetry on the average residence (and return times) can be exponentially strong *providing* the noise intensity is sufficiently weak.

## 2. General expressions for the average switching times

For completeness, we now consider the first moments of the higher order switching time distributions, i.e., the times  $\langle \tau_{j,l} \rangle$ . The average time interval  $\tau_{j,l}$  can be calculated by two ways. First by using the following expression

$$\langle \tau_{j,l} \rangle = \int_0^\infty \tau_{j,l} P_{j,l}(\tau_{j,l}) d\tau_{j,l},$$

and second by summing the average residence times

$$\langle \tau_{j,l} \rangle = \sum_{k=1}^j \langle \tau_{k,l} \rangle.$$

Since there are two kinds of distribution for odd  $j$  and two kinds of distribution of the times for even  $j$ , there are four expression for the average times,

$$\langle \tau_{2r+1,1} \rangle = [(r+1)\alpha_p + r\alpha_q] \frac{T}{2} + \delta_{s1m} + \delta_{f1m}, \quad (57)$$

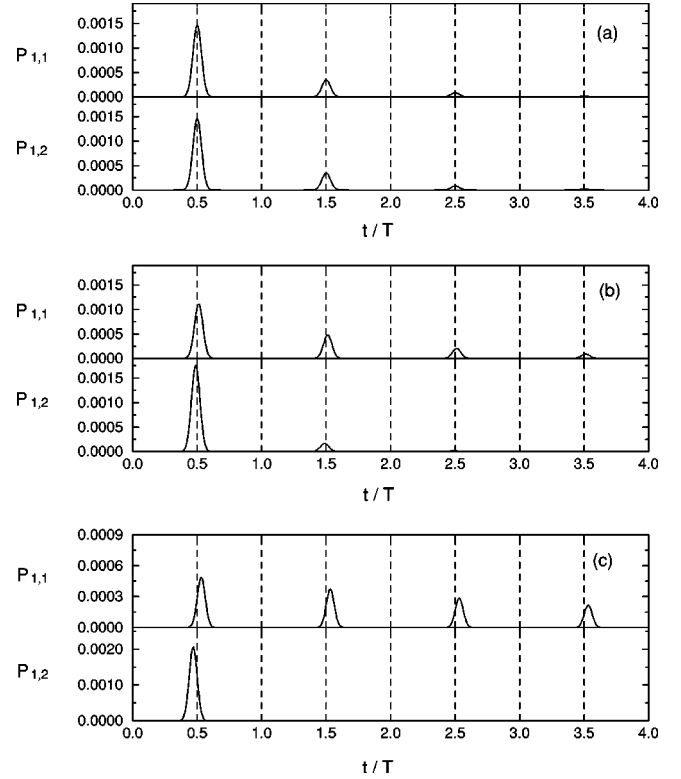


FIG. 2. The residence time probability densities  $P_{1,1}$  and  $P_{1,2}$ . The parameters are  $a=1.0$ ,  $b=1.0$ ,  $A=0.34$ ,  $\Omega=0.001$ , and  $D=0.003$ , (a)  $c=0.0$ , (b)  $c=0.005$ , (c)  $c=0.015$ .

$$\langle \tau_{2r+1,2} \rangle = [r\alpha_p + (r+1)\alpha_q] \frac{T}{2} + \delta_{s2m} + \delta_{f2m}, \quad (58)$$

$$\langle \tau_{2r,1} \rangle = (\alpha_p + \alpha_q) \frac{rT}{2}, \quad (59)$$

and

$$\langle \tau_{2r,2} \rangle = (\alpha_p + \alpha_q) \frac{rT}{2}. \quad (60)$$

It is easy to see that the difference of the average times with odd  $j$  is equal to the difference of the average residence times:

$$\begin{aligned} \Delta T_{2r+1} &= \langle \tau_{2r+1,1} \rangle - \langle \tau_{2r+1,2} \rangle \\ &= (\alpha_p - \alpha_q) \frac{T}{2} + 2(\delta_{s1m} + \delta_{f1m}) = \Delta T, \end{aligned} \quad (61)$$

and the average times with even  $j$  are identical

$$\langle \tau_{2r,1} \rangle = \langle \tau_{2r,2} \rangle.$$

## IV. RESULTS AND DISCUSSION

### A. Residence time distributions and average residence times

Plots of the residence time distribution are shown in Figs. 2 and 3. Figure 2 shows the distributions for three different

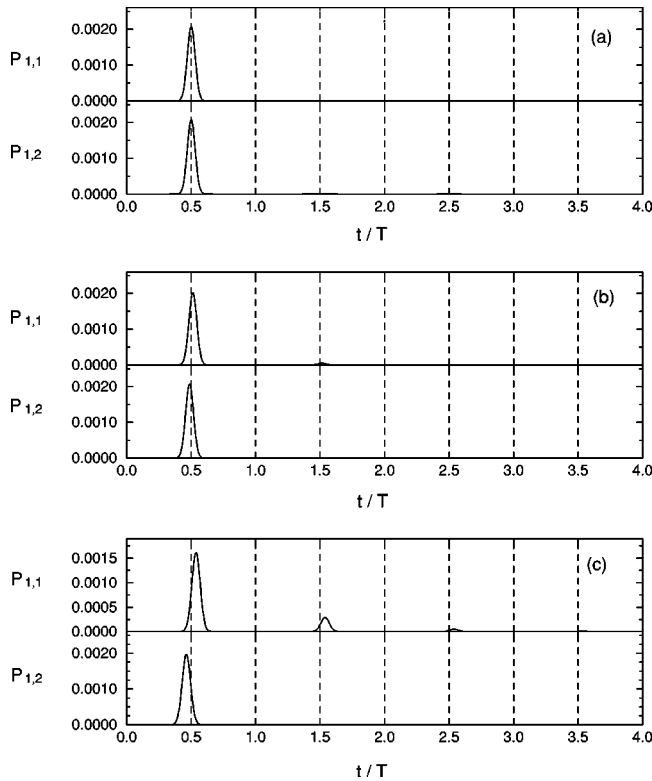


FIG. 3. The residence time probability densities  $P_{1,1}$  and  $P_{1,2}$ . The parameters are  $a=1.0$ ,  $b=1.0$ ,  $A=0.34$ ,  $\Omega=0.001$ , and  $D=0.0045$ , (a)  $c=0.0$ , (b)  $c=0.005$ , (c)  $c=0.015$ .

values of  $c$  [increasing  $c$  from (a)–(c)]. Figure 3 is for the same values of  $c$  but at a higher noise intensity. These distributions, calculated using Eqs. (37) and (38), consist of a sequence of peaks that are approximately Gaussian with variance  $\sigma_{f1}^2 + \sigma_{s1}^2$ , where  $\sigma_{f1}^2$  and  $\sigma_{s1}^2$  are given by Eqs. (A7) and (A9), respectively (note  $\sigma_{f2}^2 = \sigma_{s1}^2$ ). The widths of the peaks in  $P_{1,1}$  are always the same as those in  $P_{1,2}$ . For the symmetric case [Figs. 2(a) and 3(a)], the peaks are positioned exactly at intervals of  $(m+1/2)T$ . However, a non-zero value of  $c$  causes the peaks to shift. For positive  $c$  all the peaks in  $P_{1,1}$  are shifted (by the same amount) to the right by  $\delta_{s1m} + \delta_{f1m}$ , where  $\delta_{s1m}$  is given by Eq. (A10) (noting  $\delta_{s1m} = -\delta_{f2m}$ ) and  $\delta_{f1m}$  is given by Eq. (A4). The shifts in  $P_{1,2}$  are identical in magnitude but to the left. For negative  $c$  the situation reverses (i.e., peaks shift left in  $P_{1,1}$  and right in  $P_{1,2}$ ). These effects are demonstrated more clearly in Fig. 4 that shows a comparison between the theory and the results of a digital simulation of system (1). The theory (solid line) and simulation results (jagged line) are almost indistinguishable. For clarity, the inset shows a comparison of the first two peaks of  $P_{1,1}$  and  $P_{1,2}$ . This clearly demonstrates the shifts discussed above.

Another effect of the asymmetry is to desynchronize the response and external forcing. For a suitable choice of parameters it is possible to make the system switch every half period with probability close to unity—such a situation is shown in Fig. 3(a). We refer to this state as pseudosynchronized (or effectively synchronized with the periodic force [22]). Increasing the asymmetry is seen to result in additional

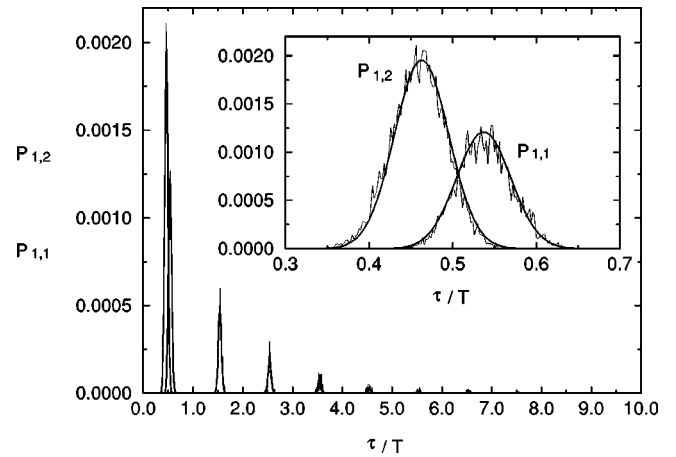


FIG. 4. Comparison of the theoretical residence time probability densities  $P_{1,1}$  and  $P_{1,2}$  (solid lines) to results obtained from a digital simulation of system (1) (jagged lines). The parameters are  $a=1.0$ ,  $b=1.0$ ,  $A=0.34$ ,  $\Omega=0.001$ ,  $D=0.0039$ , and  $c=0.015$ . The inset shows the first two peaks only.

peaks appearing in  $P_{1,1}$ . This indicates that the periodicity of the response is broken and thus the response is partially desynchronized with respect to the driving field. Such a desynchronization leads to a large increase in the average residence time  $\langle \tau_{1,1} \rangle$ . It can be seen that there is little effect on  $\langle \tau_{1,2} \rangle$ . This result is fairly intuitive. However, less obvious is that this desynchronization (and associated large change in residence time) can be achieved for extremely small asymmetries. This will be discussed in more detail below.

The results for the average residence times and their difference  $\Delta T$  are shown in Fig. 5. Figure 5(a) shows the dependence of the residence times  $\langle \tau_{1,1} \rangle$  and  $\langle \tau_{1,2} \rangle$  on noise intensity for three different asymmetries. From this figure it can be seen, as one would expect, that the average residence times increase monotonically (approximately exponentially) with decreasing noise intensity. In the limit of large  $D$ , all curves tend to 0.5, i.e., at sufficiently large noise intensities the response becomes pseudosynchronized to the external field. At larger values of  $D$  (not shown) further decrease in the residence times will occur, but this is outside the range of validity of the theory. It can also be seen that the effect of asymmetry is to cause the residence times to differ—the larger the asymmetry, the larger the difference. This effect is shown more clearly in Fig. 5(b) where the difference  $\Delta T/T$  between the residence times is shown as a function of normalized noise intensity. Clearly, at a fixed value of noise, increasing  $c$  leads to a (large) change in  $\Delta T$ . However, it can be seen that the effect of the asymmetry is reduced as the noise intensity is increased. This effect can also be clearly seen by comparing Figs. 2(c) and 3(c). Figure 2(c) shows the case where state 2 is pseudosynchronized (i.e.,  $P_{1,2}$  has a single peak) but state 1 is multi-peaked. With an increase in noise, as shown in Fig. 3(c), the multiple-peak structure in  $P_{1,1}$  is reduced—thus, reducing the difference between the residence times. We note that the results in Fig. 5(b) are strikingly similar to results obtained in Ref. [6] for a suprathreshold bias signal.

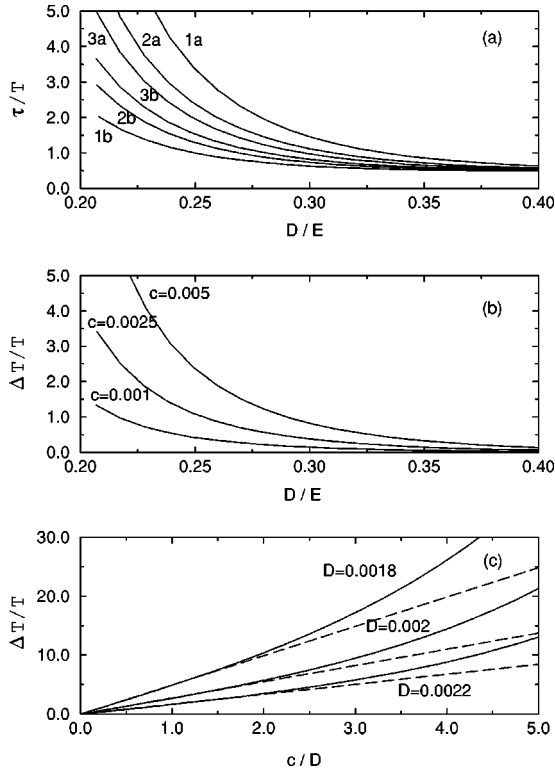


FIG. 5. (a) The average residence times as a function of the normalized noise intensity  $D/E$ , where  $E = V(x_s(0), 0) - V(x_1(0), 0)$ . The lines 1a, 2a, and 3a correspond to the residence time  $\tau_{1,1}$  with the parameters  $c=0.005$ ,  $c=0.0025$ , and  $c=0.001$ , respectively. Lines 1b, 2b, and 3b correspond to the residence time  $\tau_{1,2}$  with the parameters  $c=0.005$ ,  $c=0.0025$ , and  $c=0.001$ . The theory is calculated from expressions (39) and (40). (b) The difference between the average residence times as a function of the noise intensity  $D/E$  and (c) as a function of the parameter  $c/D$ . The solid lines were obtained by using Eq. (41). The parameters are  $a=1.0$ ,  $b=1.0$ ,  $A=0.34$ , and  $\Omega=0.001$ . The dashed lines are the approximation (46).

The reason why increasing the noise intensity reduces the effect of the asymmetry can be understood by considering Fig. 5(c) that plots  $\Delta T/T$  as a function of  $c/D$ . The solid lines are the full theory and the dashed lines show the approximations for  $|c/D| \ll 1$ . Clearly, at sufficiently small  $|c/D|$ ,  $\Delta T$  displays a linear dependence as predicted in Eq. (46). Furthermore, it is easy to see from Eq. (46) that

$$\Delta T \propto \exp\left(\frac{\Delta U}{D}\right) \frac{c}{D} \frac{1}{\sqrt{D}},$$

i.e.,  $c$  is multiplied by a factor that depends exponentially on  $1/D$ . Thus, increasing  $D$  results in an almost exponential decrease in the effective value of  $c$ .

The parameter  $c/D$  arises directly from the dc perturbation to the potential  $V(x, t)$ . This perturbation contributes an additional factor of  $c\Delta_x/D$  to the potential barrier height, where  $\Delta_x$  measures the distance between the position of the potential minimum and maximum. This, in turn, leads to an additional factor of  $\exp(c\Delta_x/D)$  appearing in the expressions

for the transition rates (8). Consequently, the important quantity for determining the effect asymmetry has on the dynamics is  $c\Delta_x/D$ . However, for the Duffing potential studied here,  $\Delta_x$  is  $O(1)$  and hence this reduces to simply  $c/D$ . Roughly speaking, it can be expected that the condition  $|c/D| \ll 1$  will lead to linear perturbations to the dynamics while, in the opposite limit of  $|c/D| \gg 1$ , the dynamics can be expected to depend exponentially on the asymmetry. This picture is borne out in Fig. 5(c) where the linear approximation is seen to hold for values of  $c/D \sim 1$  or less, while the behavior becomes approximately exponential for large values of  $c/D$ .

## B. Using $\Delta T$ as a detection tool

This work was, in part, inspired by recent theoretical and experimental work [6,23] on developing residence time distribution (RTD)-based readout schemes for a class of nonlinear dynamic sensors; the sensor under consideration was a prototype fluxgate magnetometer which uses a wound ferromagnetic core to detect weak dc magnetic fields in the presence of hysteresis. The core is driven by a known time-sinusoidal magnetic field and the shift,  $\Delta T$ , in the mean residence times taken as a measure of the (unknown) dc signal. While the idea of exploiting the asymmetry as a detection tool using spectral techniques [10,11,2–4] is not new, the RTD-based technique is relatively simple to implement, usually requiring a simple counting circuit to keep track of the threshold crossing events and to maintain a running average of the residence times. A simple analog counter performs this function quite well. It is also of interest to reduce the on-board power requirements as far as possible in most applications, in turn this implies using a low-amplitude, low-frequency bias signal. At low power, spectral techniques can be difficult to implement. Also, conventional readout schemes often employ a feedback or nulling circuit technique that leads to complicated electronics; in turn, this increases the noise floor in the device. In recent work [6], the use of a somewhat suprathreshold bias signal in a RTD-based readout was investigated. Amongst the findings of this work was the realization that a sinusoidal bias waveform might not be optimal; far greater sensitivity (or resolution) could be obtained via alternate (nonsinusoidal) bias waveforms. It can be shown [5] that, ideally, one obtains the optimal response with zero bias signal, i.e., very low on-board power (used mainly for the readout circuitry); however, this scenario is unlikely to be realizable in many operational scenarios due to the (usually short) observation time. Hence, it would be useful to operate the sensor with a bias signal that is not zero, but also not very strong.

These results are consistent with the ones obtained in this study. Figure 6 shows results of  $\Delta T$  against the amplitude  $A$  of the periodic field. Clearly,  $\Delta T$  is seen to increase (approximately exponentially) as  $A$  is reduced. This would seem to indicate that to maximize  $\Delta T$  the amplitude should be taken as small as possible. However, reducing  $A$  will also result in a reduction of the average transitions rate and, thus, a compromise is required;  $A$  should not be so small that unreasonably long averaging times are required to obtain good statis-

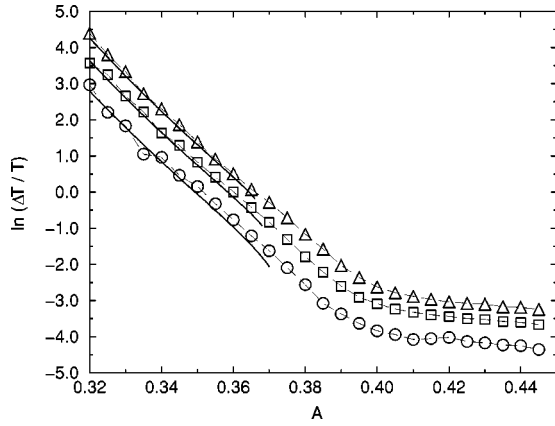


FIG. 6. The average difference between the residence times  $\Delta T$  as function of  $A$ . The data points were obtained from numerical simulation of Eq. (1) for three different values of  $c$ ; these were (circles)  $c=0.005$ , (squares)  $c=0.01$ , and (triangles)  $c=0.015$ . The solid lines are the theoretical results obtained from Eq. (41). The parameters were  $\Omega=0.01$ ,  $D=0.0039$ . The numerical results extend into the range where the periodic field is suprathreshold—this occurs approximately at  $A=0.39$

tics, but should not be so large as to reduce  $\Delta T$  to a minimum.

Ultimately, however, the extent to which weak dc target signals can be detected using this idea depends crucially on how sensitive the system dynamics are to the induced asymmetry. Weak signals demand large sensitivity; this sensitivity should not be gained at the expense of a reduced output signal-to-noise ratio. Our studies suggest that a possible candidate as a working regime could be the regime  $|c/D| \gg 1$  ( $D \ll |c| \ll 1$ ). In this regime, the system acts as an exponential amplifier. However, a possible disadvantage of working in this regime is that the observation time required to get good statistics may outweigh any advantages. As stated above, this is clearly a function of the particular operational scenario at hand.

### C. Return time distributions and average return times

Plots of the return time distribution are shown in Figs. 7 and 8. Figure 7 shows the distributions for three different values of  $c$  [increasing  $c$  from (a)–(c)]. Figure 8 is for the same values of  $c$  but at a higher noise intensity. These distributions, calculated using Eqs. (47) and (48), consist of a sequence of Gaussian peaks positioned exactly at intervals of  $mT$ . It can be seen that there are a number of notable differences between the effect of asymmetry on the return time density and the residence time distributions. The main difference is that the peaks in the return time distributions are *not* shifted by the asymmetry. The only effect of asymmetry is to change the widths of the peaks and to alter their height. Another difference is that, unlike the residence time distributions, the widths of the peaks are different between those in  $P_{2,1}$ , which have a width of  $2\sigma_{s1}$ , and those in  $P_{2,2}$  which have a width of  $2\sigma_{s2}$ . The variances  $\sigma_{s1}^2$  and  $\sigma_{s2}^2$  are given by Eqs. (A9) and (A7), respectively (noting  $\sigma_{f1}^2 = \sigma_{s2}^2$  and  $\sigma_{f2}^2 = \sigma_{s1}^2$ ). The difference in the widths is clearly shown in

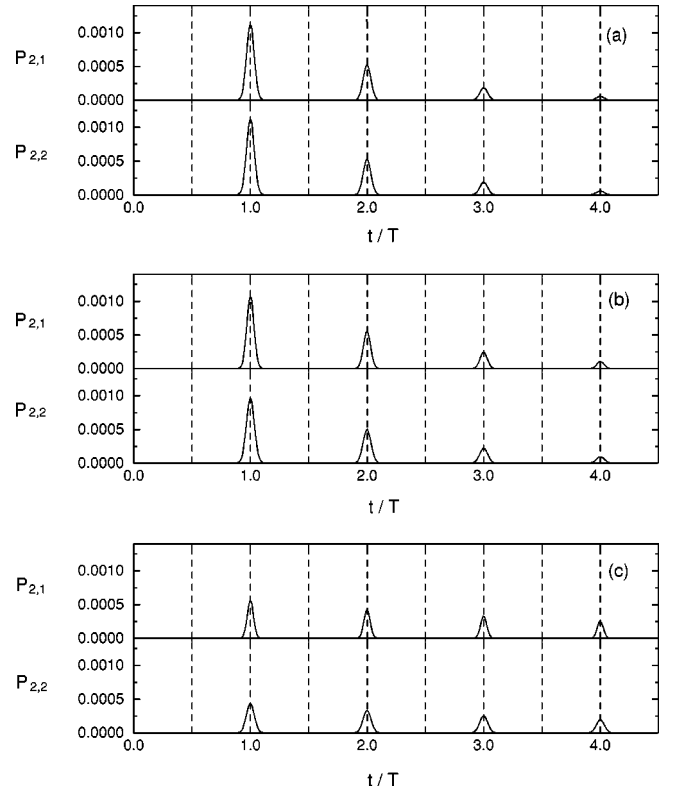


FIG. 7. The return time probability densities  $P_{2,1}$  and  $P_{2,2}$ . The parameters are  $a=1.0$ ,  $b=1.0$ ,  $A=0.34$ ,  $\Omega=0.001$ , and  $D=0.003$ , and (a)  $c=0.0$ , (b)  $c=0.005$ , (c)  $c=0.015$ .

Fig. 9 (inset). This figure shows a comparison between a theoretically calculated return time density (solid line) and one obtained from the digital simulation (jagged line). Just as with the residence time, the two sets of results are barely distinguishable.

The effect of the asymmetry on the peak widths of the return time distributions can be understood by considering the full sequence of transitions comprising the return times. We have two possible transition scenarios: transitions  $1 \rightarrow 2$ ,  $2 \rightarrow 1$ , and finally,  $1 \rightarrow 2$ , and the opposite sequence,  $2 \rightarrow 1$ ,  $1 \rightarrow 2$ , and finally,  $2 \rightarrow 1$ . Now the smearing giving rise to the finite width of the peaks only occurs on the first and last transition (see previous discussion). Consequently, for the first transition sequence, the smearing arises from two  $1 \rightarrow 2$  transitions, while it arises from two  $2 \rightarrow 1$  transitions in the second case. These two transitions have different smearing associated with them and hence the widths of the peaks in  $P_{2,1}$  and  $P_{2,2}$  will be different. Similar arguments also explain why the widths of the peaks in the residence time distributions are the same.

Another property of the return time distributions is that  $P_{2,1}$  and  $P_{2,2}$  have exactly the same rate of decay (envelope) and thus have identical average return times. This obviously has to be the case because the average return time is the sum of the two residence times, i.e.,  $\langle T \rangle = \langle \tau_{1,1} \rangle + \langle \tau_{1,2} \rangle$ . Clearly, it does not matter in which state the system started, the average return time must always be the same. The average return times are shown in Fig. 10. The solid lines in both Figs. 10(a) and (10(b)) are the full theory that is compared to

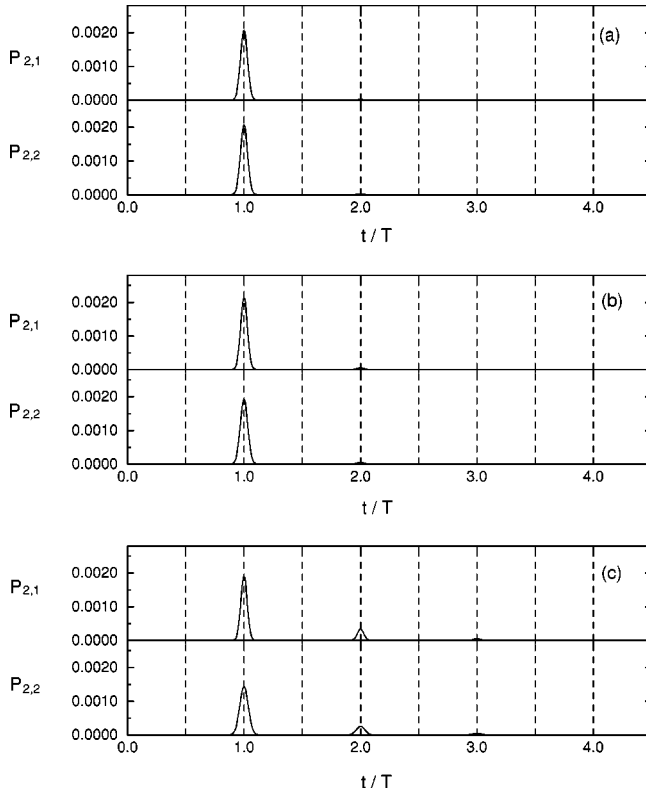


FIG. 8. The return time probability densities  $P_{2,1}$  and  $P_{2,2}$ . The parameters are  $a=1.0$ ,  $b=1.0$ ,  $A=0.34$ ,  $\Omega=0.001$ ,  $D=0.0045$ , and (a)  $c=0.0$ , (b)  $c=0.005$ , (c)  $c=0.015$ .

two different approximations. In Fig. 10(a) it is compared to the approximations valid for  $|c/D| \gg 1$ , Eqs. (55) and (56), and in Fig. 10(b) it is compared to the approximation valid for  $|c/D| \ll 1$ , Eq. (54). Figure 10(a) clearly demonstrates that, just like the residence times, the return time is seen to depend exponentially on  $c$  when  $|c/D| \gg 1$ . The full theory is almost indistinguishable from the exponential approximation when  $|c/D| > 5$ . Similarly, in the opposite limit  $|c/D| \ll 1$ , the parabolic approximation (54) gives accurate results when  $|c/D| < 2$ .

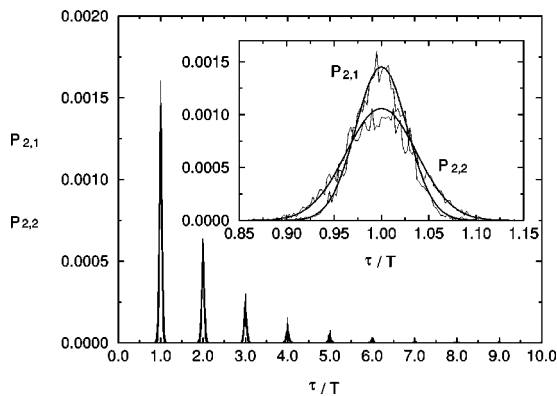


FIG. 9. Comparison of the return time probability densities  $P_{2,1}$  and  $P_{2,2}$  (solid lines) to results obtained from a digital simulation of system (1) (jagged lines). The parameters are  $a=1.0$ ,  $b=1.0$ ,  $A=0.34$ ,  $\Omega=0.001$ ,  $D=0.0039$ , and  $c=0.015$ .

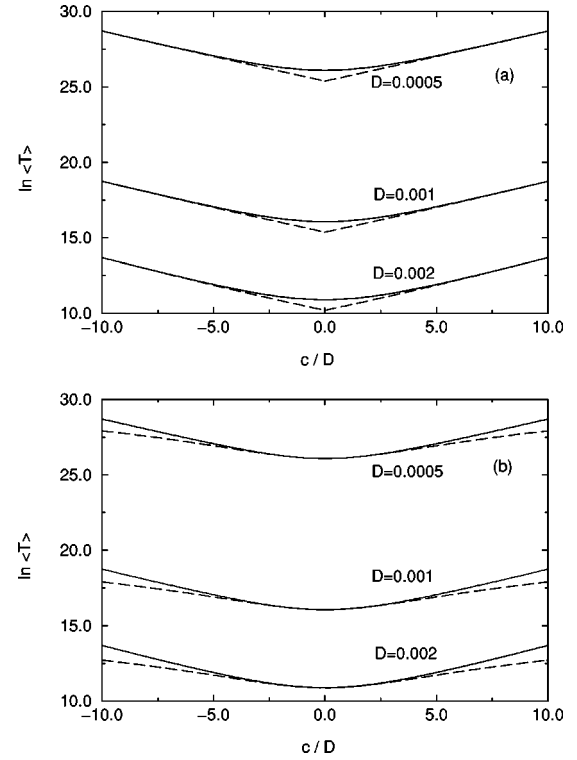


FIG. 10. The logarithms of the average return time as a function of the parameter  $c$ . The solid lines are the full theory obtained using Eq. (53). In (a) the full theory is compared to the approximations (55) and (56) shown by the dashed lines and in (b) the theory is compared to the approximation (54)—again the dashed lines are the approximation. The parameters are  $a=1.0$ ,  $b=1.0$ ,  $A=0.34$ , and  $\Omega=0.001$ .

#### D. Hierarchy of switching time distributions

Finally, the whole hierarchy of distributions are shown in Fig. 11. Figures 11(a–g) show, in order,  $P_{1,l} - P_{7,l}$ . The following general observations can be made; first, the peaks in  $P_{2r+1,l}$  ( $r=0,1,2,\dots$ ) are positioned at times  $(m+1/2)T$  and the peaks in  $P_{2r,l}$  are positioned at times  $mT$ . However, the peaks in  $P_{2r+1,l}$  are all shifted by an amount  $\delta_{s1m} + \delta_{f1m}$ ; this shift does not depend on  $r$ . Also, the decay rates of the peaks between  $P_{2r+1,1}$  and  $P_{2r+1,2}$  are generally different for nonzero asymmetry. We therefore conclude that the behavior observed for the residence time distribution ( $r=0$ ) is repeated for all other “odd” distributions, i.e.,  $P_{3,l}$ ,  $P_{5,l}, \dots$ . A similar conclusion follows for all the even distributions  $P_{4,l}, P_{6,l}, \dots$ , i.e., all the “even” distributions have the same characteristics as the return time distribution  $P_{2,l}$  ( $r=1$ ). These characteristics are that the peaks of the distributions  $P_{2r,1}$  and  $P_{2r,2}$  approximately coincide (no shift) and are of approximately the same height (same decay rate). However, just like the return time distribution, the peaks will have slightly different widths (and hence heights).

It can be seen that two main effects arise when we increase  $r$ ; first, the position of the first peaks changes, and second, that the profile (envelope) modulating the peak heights changes. The first effect is straightforward to understand. For the sake of the discussion, let us consider the distribution  $P_{6,l}$  in Fig. 11(f). In our notation, the 6 indicates

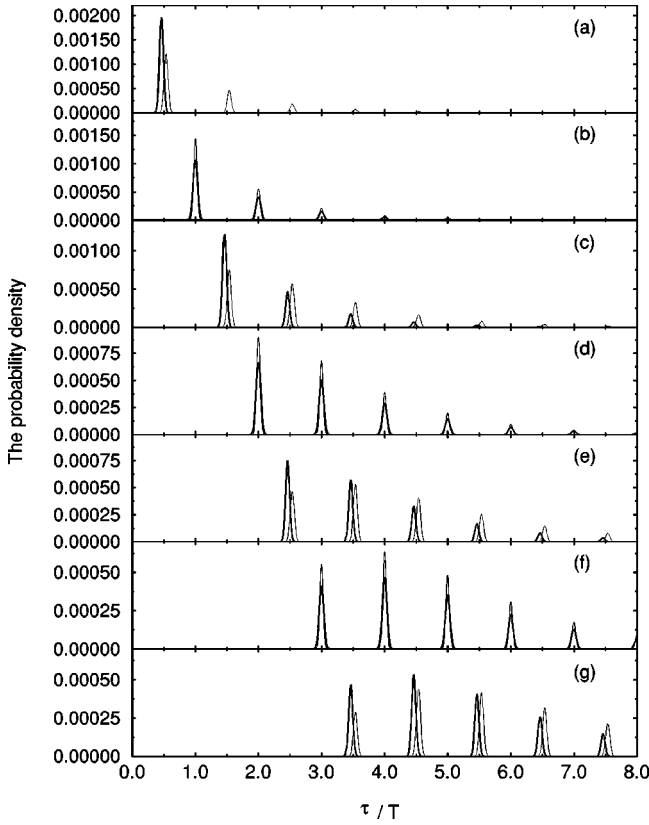


FIG. 11. The figure shows (a)  $P_{1,1}$  and  $P_{1,2}$ , (b)  $P_{2,1}$  and  $P_{2,2}$ , (c)  $P_{3,1}$  and  $P_{3,2}$ , (d)  $P_{4,1}$  and  $P_{4,2}$ , (e)  $P_{5,1}$  and  $P_{5,2}$ , (f)  $P_{6,1}$  and  $P_{6,2}$ , (g)  $P_{7,1}$  and  $P_{7,2}$ . The thin lines correspond to  $P_{1,1}$ ,  $P_{2,1}$ ,  $P_{3,1}$ ,  $P_{4,1}$ ,  $P_{5,1}$ ,  $P_{6,1}$ , and  $P_{7,1}$ . The parameters are  $a=1.0$ ,  $b=1.0$ ,  $c=0.015$ ,  $D=0.0039$ ,  $A=0.34$ , and  $\Omega=0.001$ . The probability densities were obtained using Eqs. (37), (38), (49), (50), (51), and (52).

that we are considering the time between  $6+1$  transitions. Given that under condition (9) the minimum time interval between transitions is  $T/2$ , the minimum time interval between seven transitions is  $3T$ —this time corresponds with positing of the first spike. In general, it follows that the first peak in distribution  $P_{2r+1,l}$  will occur at  $(r+1/2)T$  and in  $P_{2r,l}$  at  $rT$ .

## V. CONCLUSIONS

A comprehensive theory describing the effect of asymmetry on the switching dynamics of a bistable system has been presented. The full hierarchy of switching time distributions, and their average switching times has been obtained in the weak noise limit (limit of nonlinear response).

One of the main effects of asymmetry is to cause the residence times in the two potential wells to differ. Theoretical expressions that accurately predict the residence times and the difference between them,  $\Delta T$ , have been developed and validated. The mechanism that gives rise to a nonzero  $\Delta T$ —that is, shifts in the peaks of the residence time densities—has also been accurately described.

The most notable conclusion is that even very small asymmetries can lead to very large changes in switching dy-

namics. The important quantity that governs the effect of asymmetry was found to be the ratio of the asymmetry parameter  $c$  to the noise intensity  $D$ . For  $c/D \gg 1$  statistics, such as the residence times and  $\Delta T$  are observed to depend (approximately) exponentially on  $c$ . Consequently, a value of noise intensity can always be found (regardless of how small  $c$  is) that forces this strong dependence.

In principle, this exquisite sensitivity could be exploited to detect weak dc fields. The system could be biased using a subthreshold ac field and the noise intensity adjusted (lowered) until a measurable asymmetry-induced effect is produced. In practice, finite observation times will place a lower limit on the size of asymmetry that could be detected. Although, in principle, quantities such as  $\Delta T$  can be made arbitrarily large by reducing the noise intensity, the consequence of this is that transitions become too infrequent to enable good statistical averages to be obtained. Nevertheless, it is expected that a useful working range will exist for a suitable choice of system parameters.

A large class of nonlinear devices exhibiting dynamics underpinned by a bistable potential of (or similar to) the form discussed in this work could be operated in this manner. Our ongoing experimental work [23] on the implementation of a fluxgate magnetometer in PCB technology as a precursor to a MeMs implementation of a coupled array, as well as a magnetometer that relies on “conventional,” i.e., rod-core-based technology [6], is based on the RTD readout scheme, using nonsinusoidal bias waveforms. These experiments are also aimed at reducing the on-board power as much as possible; this might involve operation of the device in the regime indicated above, a fact that is under investigation. On a broader scale, the results of this paper are likely to find wide application in situations wherein one measures experimentally the mean residence times difference  $\Delta T$ , then wishes to use it, in a theoretical formula, to compute the dc asymmetry that produced the shift in the RTDs for the two stable steady states of the potential.

## ACKNOWLEDGMENT

We gratefully acknowledge support from the Office of Naval Research, Code 331.

## APPENDIX

The probability distribution  $P_{\delta_{f1}}(\delta_{f1})$  is given by Eq. (29),

$$P_{\delta_{f1}}(\delta_{f1}) = (1-p)^{-1} W_{12}(\delta_{f1}) \exp\left(-\int_{-T/4}^{\delta_{f1}} W_{12}(s) ds\right), \quad (\text{A1})$$

where we assume that  $P_{\delta_{f1}}(\delta_{f1})=0$  when  $|\delta_{f1}|>T/4$ . Using Eq. (14), we find

$$P_{\delta_{f_1}}(\delta_{f_1}) = (1-p)^{-1} W_{12max} \exp\left[-\frac{\delta_{f_1}^2}{2\delta t_1^2}\right] - W_{12max} \int_{-T/4}^{\delta_{f_1}} \exp\left(-\frac{s^2}{2\delta t_1^2}\right) ds. \quad (\text{A2})$$

We now proceed to obtain the time  $\delta_{f_{1m}}$  at which the distribution  $P_{\delta_{f_1}}(\delta_{f_1})$  reaches its maximum. This value represents (approximately) the average shift in the transition times away from the times  $mT/2$ . The condition of the maximum leads to the equality

$$\begin{aligned} \left. \frac{dP_{\delta_{f_1}}(\delta_{f_1})}{d\delta_{f_1}} \right|_{\delta_{f_1}=\delta_{f_{1m}}} &= (1-p)^{-1} W_{12max} \\ &\times \exp\left[-\frac{\delta_{f_1}^2}{2\delta t_1^2} - W_{12max} \int_{-T/4}^{\delta_{f_1}} \exp\left(-\frac{s^2}{2\delta t_1^2}\right) ds\right] \\ &\times \left[-\frac{\delta_{f_1}}{\delta t_1^2} - W_{12max} \exp\left(-\frac{\delta_{f_1}^2}{2\delta t_1^2}\right)\right]_{\delta_{f_1}=\delta_{f_{1m}}} = 0. \end{aligned}$$

The above equality is fulfilled when

$$-\frac{\delta_{f_{1m}}}{\delta t_1^2} = W_{12max} \exp\left(-\frac{\delta_{f_{1m}}^2}{2\delta t_1^2}\right) \quad (\text{A3})$$

or

$$-R_1 = W_{12max} \delta t_1 \exp\left(-\frac{R_1^2}{2}\right), \quad (\text{A4})$$

where

$$R_1 = \frac{\delta_{f_{1m}}}{\delta t_1}. \quad (\text{A5})$$

Using Eq. (A4), we can calculate  $\delta_{f_{1m}}$ . Then, a Taylor expansion of the exponent in Eq. (A2) about  $\delta_{f_{1m}}$  yields an approximation to the distribution  $P_{\delta_{f_1}}(\delta_{f_1})$ ,

$$\begin{aligned} P_{\delta_{f_1}}(\delta_{f_1}) &\approx \frac{W_{12max}}{1-p} \exp\left[-\frac{\delta_{f_{1m}}^2}{2\delta t_1^2} - W_{12max}\right] \\ &\times \int_{-T/4}^{\delta_{f_{1m}}} \exp\left(-\frac{s^2}{2\delta t_1^2}\right) ds - \left[\frac{\delta_{f_{1m}}}{2\delta t_1^2} + W_{12max}\right] \\ &\times \exp\left(-\frac{\delta_{f_{1m}}^2}{\delta t_1^2}\right) (\delta_{f_1} - \delta_{f_{1m}}) \\ &- \left[\frac{1}{\delta t_1^2} - W_{12max} \exp\left(-\frac{\delta_{f_{1m}}^2}{2\delta t_1^2}\right) \frac{\delta_{f_{1m}}}{\delta t_1^2}\right] \\ &\times \frac{(\delta_{f_1} - \delta_{f_{1m}})^2}{2}. \end{aligned}$$

It is easy to see that, using Eq. (A3), we can rewrite the last expression in Gaussian form

$$P_{\delta_{f_1}}(\delta_{f_1}) = \frac{1}{\sqrt{2\pi\sigma_{f_1}^2}} \exp\left(-\frac{(\delta_{f_1} - \delta_{f_{1m}})^2}{2\sigma_{f_1}^2}\right), \quad (\text{A6})$$

$$\sigma_{f_1}^2 = \frac{\delta t_1^2}{1 + R_1^2}. \quad (\text{A7})$$

We find an analogous result for  $P_{\delta_{f_2}}(\delta_{f_2})$ ,

$$\begin{aligned} P_{\delta_{f_2}}(\delta_{f_2}) &= (1-q)^{-1} W_{21}(\delta_{f_2}) \exp\left(-\int_{T/4}^{\delta_{f_2}+T/2} W_{21}(s) ds\right) \\ &= \frac{1}{\sqrt{2\pi\sigma_{f_2}^2}} \exp\left(-\frac{(\delta_{f_2} - \delta_{f_{2m}})^2}{2\sigma_{f_2}^2}\right), \end{aligned} \quad (\text{A8})$$

where

$$\sigma_{f_2}^2 = \frac{\delta t_2^2}{1 + R_2^2}, \quad (\text{A9})$$

and  $R_2$  satisfies the equation

$$-R_2 = W_{21max} \delta t_2 \exp\left(-\frac{R_2^2}{2}\right), \quad (\text{A10})$$

where  $R_2 = \delta_{f_{2m}} / \delta t_2$ .

Equations (A4) and (A10) have simple analytic solutions when the parameter  $c$  is small. In this case  $W_{12max} \delta t_1, W_{21max} \delta t_2 \ll 1$ , and Eqs. (A4) and (A10) can be rewritten as

$$-R_1 = W_{12max} \delta t_1 \left(1 - \frac{R_1^2}{2}\right), \quad R_1 < 0,$$

$$-R_2 = W_{21max} \delta t_2 \left( 1 - \frac{R_2^2}{2} \right), \quad R_2 < 0.$$

Using the designations  $I_1 = \sqrt{2\pi} W_{12max} \delta t_1$  and  $I_2 = \sqrt{2\pi} W_{21max} \delta t_2$ , we can write the solutions

$$R_1 = \frac{\sqrt{2\pi}}{I_1} - \sqrt{\frac{2\pi}{I_1^2} + 2} = \frac{\sqrt{2\pi}}{I_1} \left( 1 - \sqrt{1 + 2\frac{I_1^2}{2\pi}} \right)$$

$$\simeq \frac{\sqrt{2\pi}}{I_1} \left[ 1 - \left( 1 + \frac{I_1^2}{2\pi} \right) \right] = -\frac{I_1}{\sqrt{2\pi}}$$

and

$$R_2 \simeq -\frac{I_2}{\sqrt{2\pi}},$$

so that the final approximate solutions are

$$\delta_{f1m} = R_1 \delta t_1 = -\frac{I_1 \delta t_1}{\sqrt{2\pi}} \quad (\text{A11})$$

and

$$\delta_{f2m} = R_2 \delta t_2 = -\frac{I_2 \delta t_2}{\sqrt{2\pi}}. \quad (\text{A12})$$

Let us note that  $P_{\delta_{f1}}(\delta_{f1}) = P_{\delta_{s2}}(-\delta_{f1})$  and  $P_{\delta_{f2}}(\delta_{f2}) = P_{\delta_{s1}}(-\delta_{f2})$ , i.e.,  $\delta_{f1m} = -\delta_{s2m}$ ,  $\delta_{f2m} = -\delta_{s1m}$ , for the average values, and  $\sigma_{f1}^2 = \sigma_{s2}^2$ ,  $\sigma_{f2}^2 = \sigma_{s1}^2$  for the dispersions.

- 
- [1] A.R. Bulsara and L. Gammaitoni, Phys. Today **49**(3), 39 (1996); L. Gammaitoni, P. Hänggi, P. Jung, and F. Marchesoni, Rev. Mod. Phys. **70**, 223 (1998); *Proceedings of the International Workshop on Fluctuations in Physics and Biology: Stochastic Resonance, Signal Processing and Related Phenomena*, edited by A.R. Bulsara, S. Chillemi, R. Mannella, P.V.E. McClintock, K. Nicolis, and K. Wiesenfeld [Nuovo Cimento **17D**, 653 (1995)].
- [2] A.R. Bulsara, M.E. Inchiosa, and L. Gammaitoni, Phys. Rev. Lett. **77**, 2162 (1996).
- [3] M.E. Inchiosa and A.R. Bulsara, Phys. Rev. E **58**, 115 (1998).
- [4] M.E. Inchiosa, A.R. Bulsara, and L. Gammaitoni, Phys. Rev. E **55**, 4049 (1997).
- [5] L. Gammaitoni and A.R. Bulsara, Phys. Rev. Lett. **88**, 230601 (2002).
- [6] A.R. Bulsara, C. Seberino, L. Gammaitoni, M.F. Karlsson, B. Lundqvist, and J.W.C. Robinson, Phys. Rev. E **67**, 016120 (2003).
- [7] A.P. Nikitin, N.G. Stocks, and A.R. Bulsara, Phys. Rev. E (to be published).
- [8] T. Zhou and F. Moss, Phys. Rev. A **41**, 4255 (1989); T. Zhou, F. Moss, and P. Jung, *ibid.* **42**, 3161 (1990).
- [9] R. Lofstedt and S.N. Coppersmith, Phys. Rev. E **49**, 4821 (1994).
- [10] R. Bartussek, P. Jung, and P. Hänggi, Phys. Rev. E **49**, 3930 (1994).
- [11] P. Jung and R. Bartussek, in *Fluctuations and Order: The New Synthesis*, edited by M. Millones (Springer, New York, 1988).
- [12] F. Marchesoni, F. Apostolico, and S. Santucci, Phys. Rev. E **59**, 3958 (1999).
- [13] S. Bouzat and H.S. Wio, Phys. Rev. E **59**, 5142 (1999).
- [14] N.G. Stocks, Nuovo Cimento **17D**, 925 (1995).
- [15] P. Jung, Phys. Rep. **234**, 175 (1993).
- [16] B. McNamara and K. Wiesenfeld, Phys. Rev. A **39**, 4854 (1989).
- [17] M. Dykman, R. Mannella, P.V.E. McClintock, and N. Stocks, Phys. Rev. Lett. **65**, 2606 (1990); Pis'ma Zh. Eksp. Teor. Fiz. **52**, 780 (1990) [JETP Lett. **52**, 141 (1990)].
- [18] V.A. Shneidman, P. Jung, and P. Hänggi, Phys. Rev. Lett. **72**, 2682 (1994).
- [19] L. Gammaitoni, F. Marchesoni, and S. Santucci, Phys. Rev. Lett. **74**, 1052 (1995).
- [20] M.H. Choi, R.F. Fox, and P. Jung, Phys. Rev. E **57**, 6335 (1998).
- [21] A. Longtin, A. Bulsara, and F. Moss, Phys. Rev. Lett. **67**, 656 (1991).
- [22] V.S. Anishchenko, A.B. Neiman, F. Moss, and L. Schimansky-Geier, Usp. Fiz. Nauk **69**, 7 (1999) [Sov. Phys. Usp. **42**, 7 (1999)]; A. Neiman, A. Silchenko, V. Anishchenko, and L. Schimansky-Geier, Phys. Rev. E **58**, 7118 (1998).
- [23] B. Ando, S. Baglio, A. Bulsara, and L. Gammaitoni (unpublished).